INVESTIGATION OF CO_2 SEQUESTRATION OPTIONS FOR ALASKAN NORTH SLOPE WITH EMPHASIS ON ENHANCED OIL RECOVERY

By

Santosh Bramhadev Patil

RECOMMENDED:

Advisory Committee Chair

Chair, Department of Petroleum Engineering

APPROVED:

Dean, College of Engineering & Mines

Dean of the Graduate School

August 21, 2006

Date

INVESTIGATION OF CO_2 SEQUESTRATION OPTIONS FOR ALASKAN NORTH SLOPE WITH EMPHASIS ON ENHANCED OIL RECOVERY

A

THESIS

Presented to the Faculty

of the University of Alaska Fairbanks

in Partial Fulfillment of the Requirement

for the Degree of

MASTER OF SCIENCE

By

Santosh Bramhadev Patil, M.S.

Fairbanks, Alaska

August 2006

Abstract

Carbon dioxide (CO_2), the main component of greenhouse gases, is released into the atmosphere primarily by combustion of fossil fuels like coal and oil. Due to a conspicuous lack of any CO_2 sequestration studies for Alaskan North Slope (ANS), the study of CO_2 sequestration options will open new avenues for CO_2 disposal options, such as viscous oil reservoirs and coal seams, on the ANS. This study focuses on the investigation of CO_2 storage options by screening ANS oil pools amenable to enhanced oil recovery, evaluating phase behavior of viscous oil and CO_2 mixture, and simulating enhanced oil recovery by CO_2 flooding, and migration of CO_2 in saline aquifer.

Phase behavior studies revealed that CO_2 gas was partially miscible with West Sak, at the pressure closer to the reservoir pressure. Compositional simulation of CO_2 flooding for a five-spot West Sak reservoir pattern showed an increase in percent recovery with an increase in pore volume injected, but at the expense of an early breakthrough. Sensitivity analysis of CO_2 flooding project was found to be strongly dependent on the variables such as oil price and discount rate. Investigation of supercritical CO_2 injection in saline formation didn't increase temperature in the permafrost region.

Table of Contents

Table of Contents (cont'd)

List of Figures

List of Figures (cont'd)

List of Tables

Acknowledgements

First and foremost, I would like to offer my gratitude to Mr. Shirish Patil for his guidance and encouragement during the course of this work as my advisor. I am very thankful to the committee members, Drs. Abhijit Dandekar and Santanu Khataniar, for their valuable advice and support. I am indebted to all of my family and friends for their help and support.

The material was prepared with financial support from the Arctic Energy Office-National Energy Technology Lab, US Department of Energy. Their support is highly appreciated. The opinions, findings, conclusions, and recommendations expressed herein are those of the author and do not necessarily reflect the views of the US Department of Energy.

Chapter 1

Introduction

1.1 Overview

Carbon dioxide, which is an important greenhouse gas (GHG), is predominantly released in the atmosphere by burning fossil fuels. According to the Energy Information Administration (2005), the total CO_2 emission for the United States (US) was 5,973 million tons, which was the largest portion contributing to the total GHG emission of 7,122 million tons.

In the year 2001, the state of Alaska emitted around 43.20 million tons of CO_2 from a sundry of sources such as transportation, industries, commercial, and residential sections (EIA, 2001). The traditional drilling for fossil fuels on the ANS is released approximately 8 million tons of CO_2 after major gas sales (Figure1.1).

The impact of global warming on the arctic environment has become evident by the rapid melting of ice glaciers. Their relation between global warming and the arctic environment can be summarized as follows:

- Trapping of heat due to released CO_2 can increase average winter temperatures
- Reduction in the extent of the summer ice pack in the Arctic Ocean
- Either change could further accelerate warming

- Changes in temperature could substantially reduced the winter drilling window, thus threatening oil and gas developmental drilling and related activities

A method like CO_2 storage in geological formations is an important sequestration option to decreasing concentration of CO_2 in the environment. Other synergies such as, recovery of viscous oil by CO_2 flooding could also be very attractive and economical. Bachu and Shaw (2003) defined geological sequestration of CO_2 as capturing CO_2 from anthropogenic sources, followed by disposal in geological media. A typical CO_2 sequestration project includes i) capture of CO_2 from point sources like power plants and natural gas sales by chemical techniques such as amine absorption, ii) compression of gas, iii) transportation through a corrosion-resistant pipeline or tanker, and iv) storage in the potential geological sinks. Figure 1.2 represents a typical CO_2 sequestration scheme.

Other than sequestering CO_2 gas for enhanced oil recovery (EOR), CO_2 can also be sequestered: i) in depleted oil and gas reservoirs, ii) through replacing methane by CO_2 in deep coal beds, iii) deep saline aquifers (Bachu and Stewart, 2002). There are three important mechanisms by which CO_2 is geologically sequestered, which are: hydrodynamic trapping, solubility trapping, and mineral trapping (Kovscek, 2002). Sequestration of CO_2 on the ANS to produce viscous oil (immiscible/miscible displacement) and coalbed methane by CO_2 injection will

lead to increased oil and gas production, respectively, to meet the current energy demands by taking advantage of available infrastructure on the ANS. On the ANS, West Sak and Ugnu sands are amenable to CO_2 flooding due to the viscous nature of oil, thus supplying additional drive created due to viscosity reduction, swelling of oil, and in some cases immiscible or miscible displacement on CO_2 injection. Enhanced oil recovery can start after a secondary recovery process or at any time during the productive life of an oil reservoir to improve fluid displacement. In this study, term EOR is used in conjunction with improved viscous oil recovery by CO_2 injection.

Figures 1.3 and 1.4, in Geographic Information System (GIS), show the sedimentary basins and coalbed along with oil and gas pools on the ANS, respectively. Availability of transportation infrastructure for building new pipeline makes the ANS very conducive to any CO_2 geological storage, provided justifiable economic feasibility is demonstrated. Moreover, successful sequestration on the ANS necessitates advances in drilling technology to develop engineered well bores to avoid communication between injected CO_2 and producer wells. Major impacts of CO_2 sequestration on the ANS to Alaska are:

- Value-added oil production is essential to protect Alaska's economic growth opportunity.

- EOR by CO_2 injection has a special significance due to its potential to tackle the issue of GHG emission in an environmental-friendly way.
- CO_2 sequestration projects will provide solutions to unlock ANS viscous oil reserves as well as different sequestration options such as saline aquifers, and depleted oil and gas reservoirs are also available.

1.2 Objectives

Lack of any current CO_2 sequestration study for ANS was the primary initiative behind the current study. The objectives of this study were to investigate different sequestration options:

1) To characterize oil pools, amenable to CO_2-EOR, by screening technique,
2) To perform phase behavior study of viscous oil and CO_2,
3) To predict the viscous oil production by injection of CO_2,
4) To calculate time value of the CO_2-EOR project,
5) And to simulate injection of supercritical CO_2 in a saline aquifer.

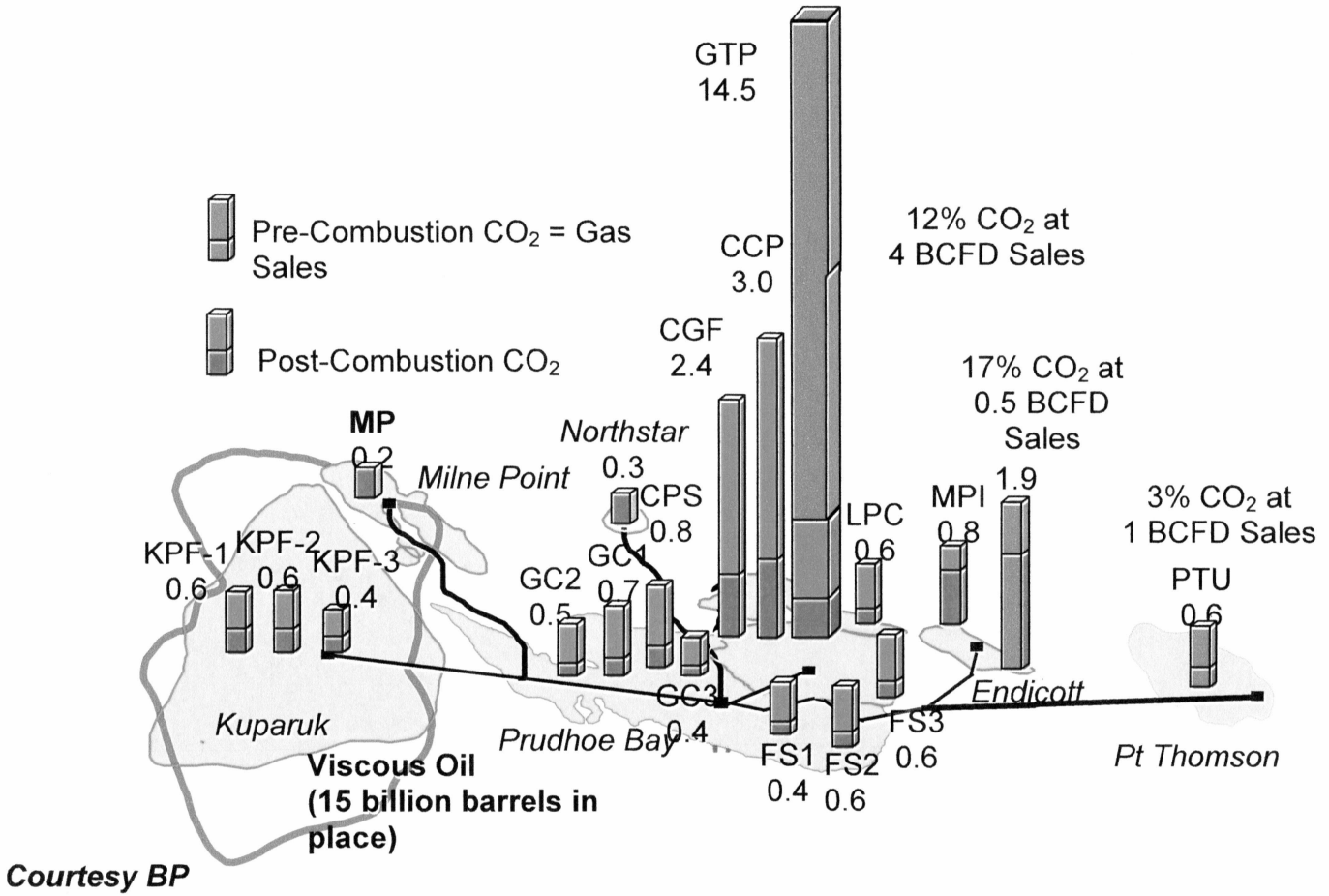

Figure 1.1: Carbon dioxide sources with and without major gas sales along with oil pools on ANS

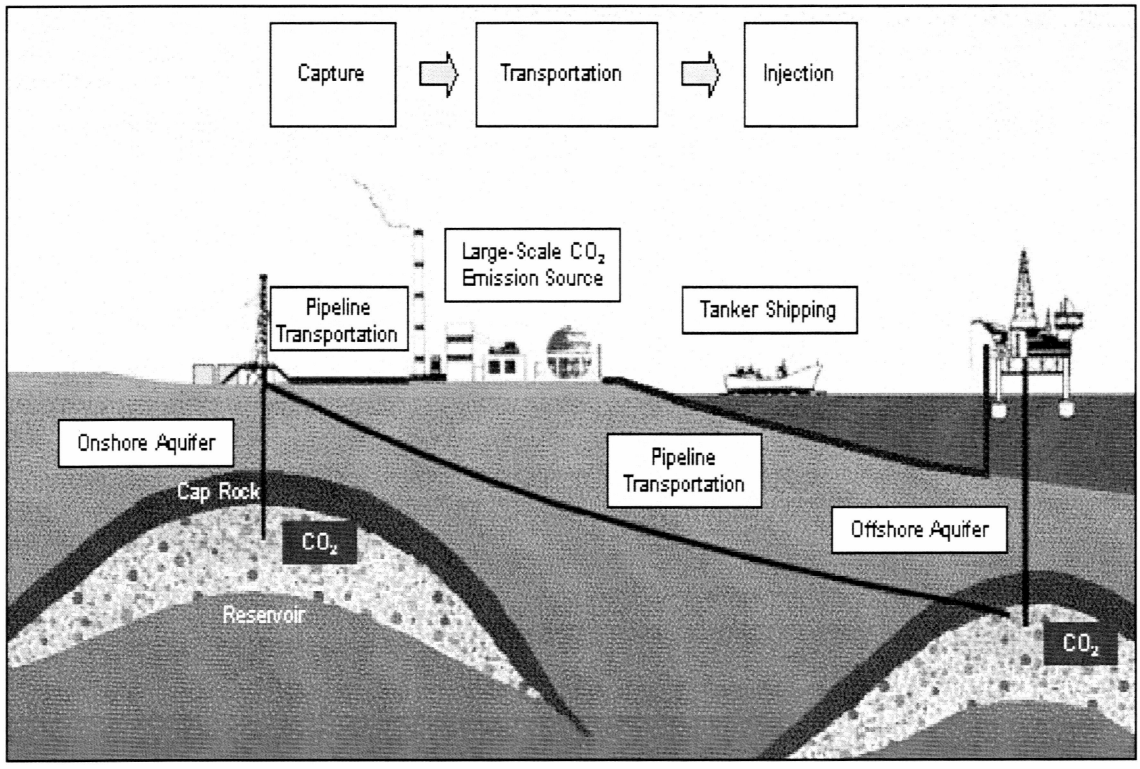

Figure 1.2: A typical CO_2 sequestration scheme (After RITE, 2004)

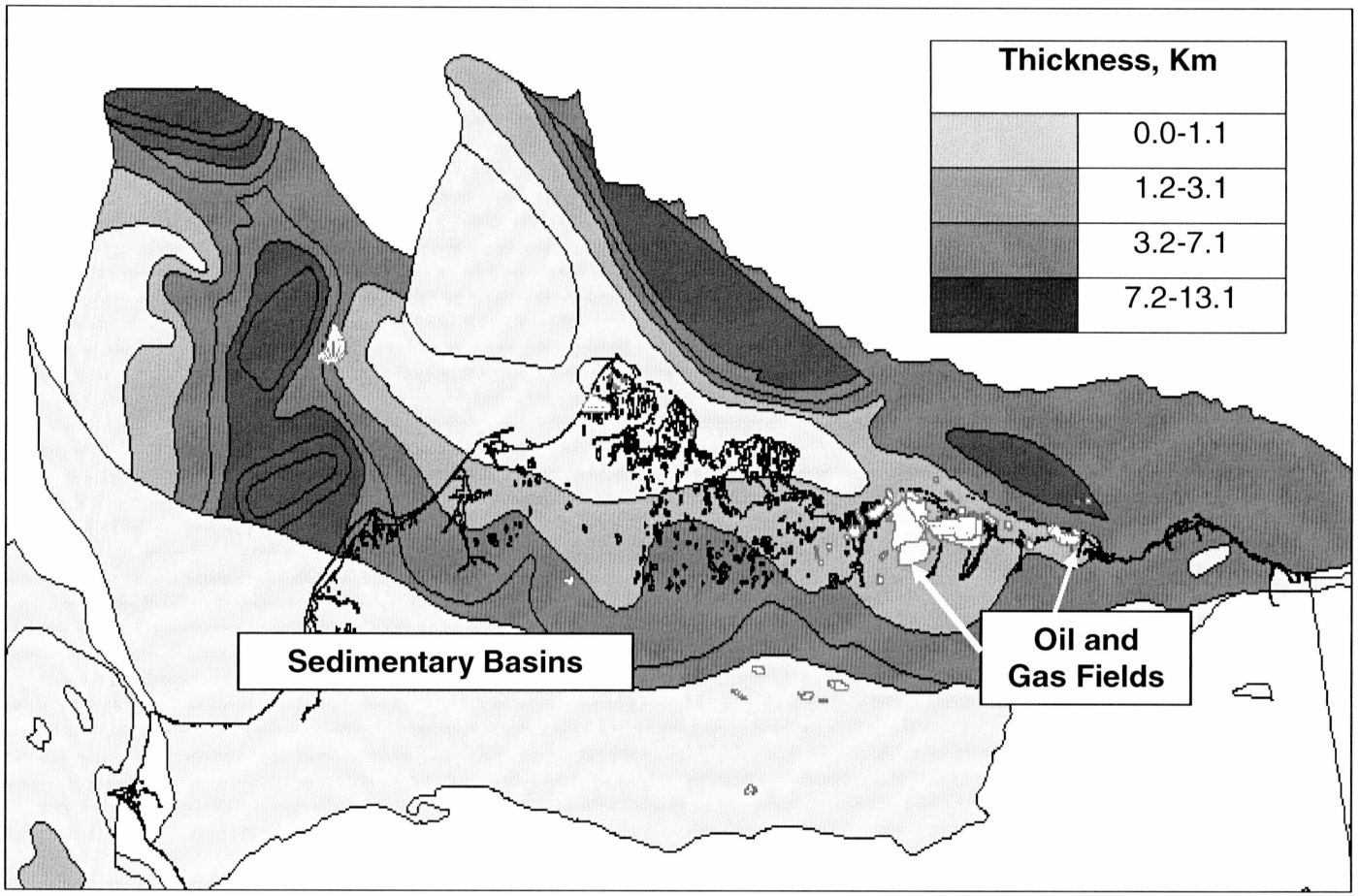

Figure 1.3: Location of sedimentary basins and their thickness on ANS

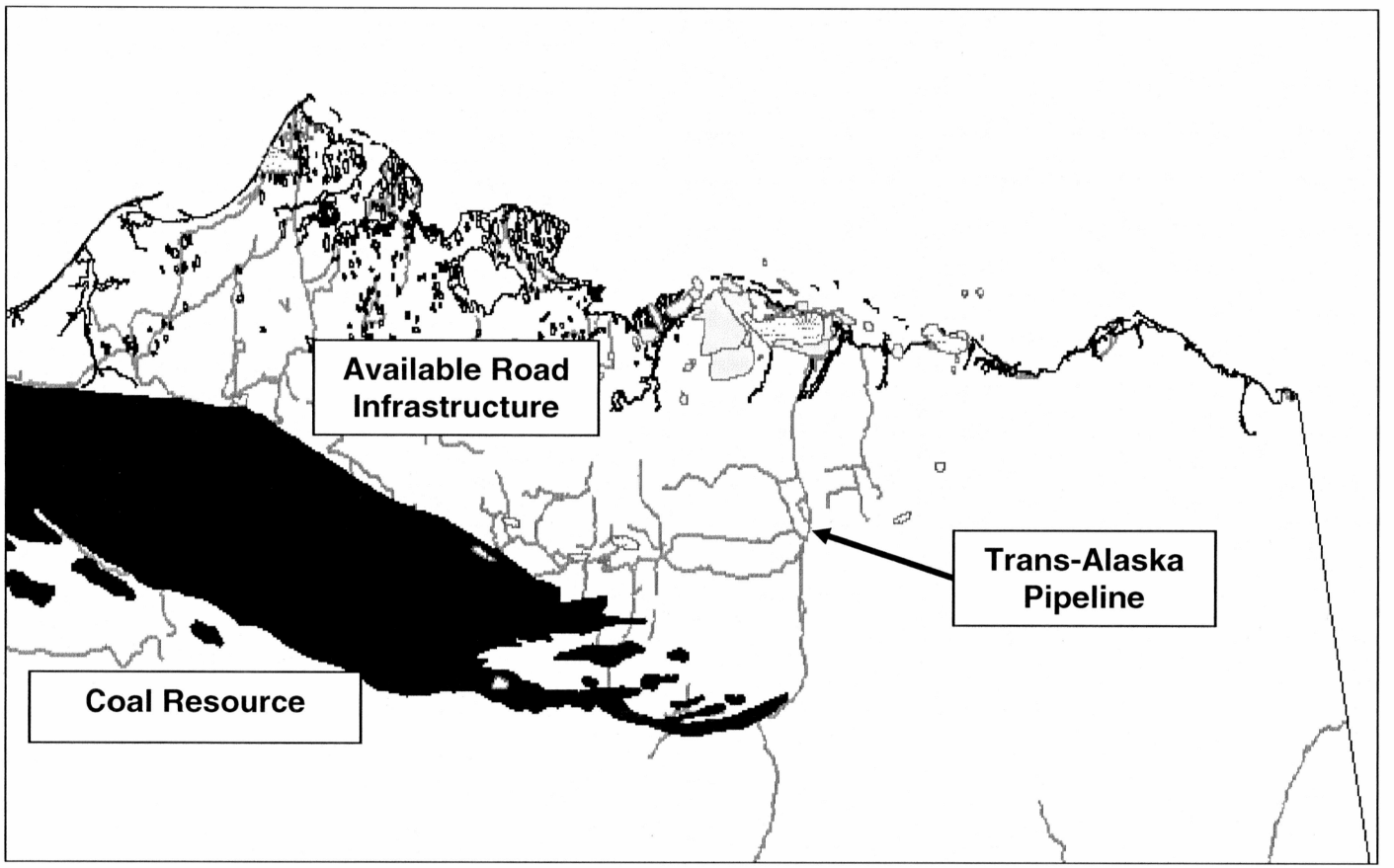

Figure 1.4: Location of coal resource and available road infrastructure on ANS for development of CO_2 sequestration project

Chapter 2

Literature Review

A plethora of studies have been performed to evaluate sequestration of CO_2 in geological formations. This chapter is divided into four major sections to include research on CO_2 sequestration, according to objectives of this study. A review of the following sections will be found in this chapter:

- Screening of oil pools
- Phase behavior study
- West Sak pool description, various field and simulation study of CO_2-EOR
- Economic analysis of CO_2-EOR
- CO_2 storage in saline aquifers

2.1 Screening of Oil Pools

The design of any EOR project involves data gathering, economic and technical feasibility studies, reservoir simulation and sensitivity analysis followed by pilot project studies. The simulation study by Bossie-Cordreanu and Gallo (2004), based on a synthetic reservoir, quantified uncertainties due to reservoir parameters in order to establish a set of guidelines to determine most suitable depleted reservoirs for sequestration. In their work, they studied the influencing parameters like API gravity, heterogeneity (Dykstra-Parson coefficient), and cap

rock integrity. The sequestration capacity was estimated through the sequestration factor for different reservoirs.

According to Klins (1984), the major task of screening potential reservoirs for EOR is accomplished by binary evaluation and project evaluation criteria. In the case of binary evaluation criteria, a comparison of important parameters with observed parameters of technically and economically successful EOR was carried out by Klins (1984). But limited number of projects and publicly available data hinders the role of screening as the sole criterion. Because of the less cumbersome application of a binary evaluation technique, it is a popular preliminary screening tool.

Rivas et al. (1992) developed a new screening tool to account for synergistic effects on process performance, which binary evaluation criterion fails to do. In that study, reservoir parameters like porosity, permeability, temperature, API gravity, oil saturation, and net pay thickness were examined. The optimum parameters, which led to the best average production rate, were obtained from simulation studies by using fully compositional, black oil, and semi-analytical models. An arbitrary heuristic function, exponentially varying function, was employed to rank different reservoirs. The value of that function depended on the difference between the properties, characteristic of the reservoir, and the optimum values of simulation studies. The optimum properties for the CO_2

injection project were found to be 37°API gravity, temperature of 160°F, permeability of 300 md, oil saturation of 60%, and porosity of 20%. Shaw and Bachu (2002) performed the same screening technique to rank the oil reservoirs in the Western Canada Sedimentary Basin. It is estimated that there is around 20 to 25 billion barrels of original-oil-in-place (OOIP) of medium and heavy oil deposits on the Alaskan North Slope (McGuire et al., 2005). Figure 1.1 of Chapter 1 shows the oil reservoirs on ANS along with CO_2 sources such as gas sales and other emissions. In the current study, screening of oil reservoirs on the ANS for their CO_2-EOR potential was based on work of Rivas et al. (1992).

2.2 Description of Equation-of-State for Phase Behavior

Minimum Miscibility Pressure (MMP) is the pressure at which injected gas and oil become miscible by multiple-contact miscible displacement. There are various generalized methods to evaluate minimum miscibility pressure for pure and impure CO_2. Ahmed (1997) briefly described various methods for determination of MMP. These methods primarily depend on the molecular weight of C_{5+}, temperature, and the weighted-composition parameter (based on partition coefficients of C_2 through C_{37} fractions).

The phase behavior of oil in CO_2 injection processes consists mainly of mass transfer as well as composition changes. Importance of tuning of equation-of-state (EOS) for prediction of phase behavior of complex process with

compositional simulator was recognized by Coats and Smart (1986) and Abrishami et al. (1997). Cubic equation-of-states like Peng-Robinson (1976) are widely used for convenient and flexible calculation of the complex phase behavior of reservoir fluids. Equation 2.1 gives the original Peng-Robinson equation-of-state (PR-EOS); this equation can indicate the relationship among pressure (P), temperature (T) and mole volume (V) of components.

$$P = \frac{RT}{V-b} - \frac{a}{V(V+b)+b(V-b)} \tag{2.1}$$

$$a = \Omega_a \frac{R^2 T_c^{\,2}}{P_c}\alpha \text{ and } b = \Omega_b \frac{RT_c}{P_c} \tag{2.2}$$

Where a and b coefficients account for the mixing in the case of multi-component mixtures and Ω_a and Ω_b are the constants.

The correction factor (α) in the equation 2.2 is dependent on the reduced temperature and quadratic function based on the acentric factor. Robinson and Peng (1978) recommended a modification to the acentric factor function to account for the heavier components; this modification will be referred as PR-EOS (1978).

EOS parameters are interdependent on the binary interaction coefficient (BIC), which represents the intermolecular forces between molecules. In spite of suitability of PR-EOS to predict phase behavior of many components, it is a far-

fetched endeavor to use PR-EOS for all components present in a fluid mixture. The need to incorporate any EOS for hydrocarbon mixtures to realize its suitability should always be weighed against the degree of inaccuracy, which is inherently expected due to the presence of heavy components. To overcome the deficiencies of EOS to predict the phase behavior of a fluid, tuning of EOS has been found to be an important practice, wherein laboratory PVT study acts as a basis for comparison to alter *a* and *b* coefficients by changing their parameters. Acentric factors, critical properties, primarily of the plus fraction, to name a few, are changed in the tuning process. Based on the consideration of methane as a dominant component and the inadequacy related to heavy fraction characterization, Abrishami et al. (1997) reported different regression variables that can be chosen in the tuning process: a) critical properties, such as P_c and T_c of heavy components since in many cases, there may not be a proper characterization of heavy fractions available; b) Ω_a and Ω_b values of methane; c) Ω_a and Ω_b values of heavy fractions; and d) BIC.

Setting of Ω_a and Ω_b, and critical properties of heavy fractions as regression variables can lead to altering *a* and *b* coefficients. While Danesh (1998) stated that the selection of BIC as a regression parameter should be dealt with by acknowledging its role as a fitting parameter rather than a physical property. It can also act effectively in changing the results predicted by tuned EOS. It should, however, be recognized that a tuned EOS is only applicable and valid for the

same system, at same temperature and pressure conditions. For CO_2 gas injection in oil, the adaptation to the compositional changes necessitates the modifications of the tuned EOS. According to Danesh (1998), all reliable experimental data must be used in tuning process.

2.3 CO_2-EOR Study

This section reviews the description of the West Sak oil pool, different displacement mechanisms of oil by CO_2 injection, laboratory, field, and various simulation studies of CO_2 displacement.

2.3.1 Description of West Sak Reservoir

Werner (1987) in detail discussed the low gravity oil zones, West Sak and Ugnu Sands, of the Kuparuk River Unit (KRU), Alaskan North Slope. According to Werner (1987), the Chevron Kavearak Point No.1 (drilled in 1969) was the very first well to encounter low-gravity oil in shallow zones of the Kuparuk River area. The depth of these shallow zones, later referred to as shallow sands, was less than 4,500 ft. The regional setting of all of the shallow oil zones is a monocline with a gentle dip of 1-2 degrees (130 feet/mile), which runs from northwest to northeast. Most of the oil was found in two zones: West Sak sands and the overlying Ugnu sands.

The gravity of oil in late Cretaceous and early tertiary marine-aged West Sak reservoir was from 16 to 22°API. The West Sak sands are very fine, unconsolidated with inter-bedded siltstones and mudstone and have areal extent of 30 miles north to south and 20 miles east to west, from the western area of Prudhoe Bay Field across the Kuparuk River Field. West Sak oil-bearing sands, similar to the Schrader Bluff Formation, are present from 3,742 to 4,040 ft, when measured at ARCO West Sak No.1 well. Geochemically, the sand grains are made up of quartz, lithic rock fragments, and feldspar with small amount of mica and glauconite.

West Sak is a highly stratified reservoir. The average stratigraphic interval thickness of the West Sak sands in the southwest is 300 ft, while in the northeast it is 200 ft. The sands are divided into upper and lower members. The lower member sands are thin-bedded, each sand range from 0.2 to 5 ft in thickness with in part amalgamated sand-rich units which range to 10 ft in thickness. Lower member sands can be laterally continuous for three to five miles. The upper member consists of two laterally distinct sands: upper sand #1 and upper sand #2, with an average thickness of 30 and 20 feet, respectively. The top of the West Sak sands ranges from 2400 ft true vertical depth subsea on the western edge of Kuparuk region to 3800 ft on the eastern edge.

Primary control on regional distribution of oil in West Sak oil pool is north-south and east-west trending faults. Temperature in West Sak oil varies from 40 to 100°F (Panda et al., 1989) due to overlaying permafrost, while pressure ranges from 1000 psi to 1800 psi due to being shallow sands. Core data indicate that the horizontal air permeability is between 10 and 800 milidarcy, with an average permeability value of 140 milidarcy, and the porosity can be as high as 0.38.

West Sak oil pool contains around 7-9 billion barrels of original-oil-in-place (McGuire et al., 2005). According to AOGCC (2003), currently the West Sak oil pool is producing continuously since December 1997. The oil production has increased from the monthly average of 19 barrels of oil per day (BOPD) to 9,300 BOPD during the first 8 months of 2004. After bringing several new wells on production in September 2004, West Sak oil production increased to its current rate of 17,000 BOPD. By December 2004, the average oil production from the 31 wells of the West Sak Pool averaged to 17,072 BOPD.

2.3.2 Theory, Field and Simulation Review

Gas injection is one of the important tertiary injection processes, which plays crucial role in enhanced oil recovery. Carbon dioxide gas, owing to its large production, non-toxic nature, role in global warming, and tendency to vaporize intermediate components, acts as an important injectant for enhanced oil recovery.

For many CO_2 flooding projects, approximately 5 to 10 Mscf (gross utilization) of CO_2 is required to recover an additional barrel of stock tank oil by miscible CO_2 displacement (Stalkup, 1984). On reaching maturity in the early 1970s, Permian Basin oil reservoirs were thought to be potential candidates for tertiary oil recovery (Holtz et al., 1999) with CO_2, obtained from natural gas produced in nearby fields. Shaw and Bachu (2002) stated that there are 76 sites worldwide that are commercially proven, of which 67 sites are in the US. CO_2 flooding is attracting attention today because it can lead to additional oil production while providing a disposal site (sink) for industrial carbon dioxide emissions. Proximity to large, high-purity source of industrial carbon dioxide emissions is an essential criterion for a feasible CO_2 flooding project, since the extraction of enough CO_2 from low-purity sources is an economically unfavorable scenario. High-purity (minimum of 80%) CO_2 can be transported to the oil field via a pipeline. Proximity of a CO_2 source to the oil reservoir is essential for economic feasibility, since it reduces the capital and operating costs of the pipeline.

The injected gas contacts reservoir oil, which causes changes in the phase behavior as well as the equilibrium conditions. Taber et al. (1997) classified the enhanced oil recovery by oil displacement mechanism. For CO_2 flooding, miscible and immiscible processes fall under vaporizing/condensing and viscosity reduction mechanisms, respectively. It is found that the miscible CO_2 injection results in higher recovery when compared with immiscible options (Srivastava et al., 1995). Immiscible CO_2 flooding, which occurs in low-pressure (below 1000

psia) reservoirs, can aid oil production by oil swelling, viscosity reduction, or solution gas drive as CO_2 gas dissolves in oil and carbonates oil (solubility of CO_2 in oil is pressure dependent phenomenon), thus increasing oil volume and reducing its viscosity. Normally, during immiscible displacement regime, presence of partial miscibility is essential for oil displacement by swelling and viscosity reduction. In the case of miscible flooding, the interfacial tension between the displacing phase and the displaced phase is minimized and consequently, the reduction in drag forces for fluid flow in porous media acts as a favorable condition for miscible flooding. Different types of mechanisms initiate the oil displacement by CO_2; nevertheless injected CO_2 may lead to a miscible front, which may be similar to the rich gas injection process. Essentially, extraction of intermediate to heavier components (C_5 to C_{30}) from oil by CO_2 can generate a favorable miscible condition.

When CO_2 is injected into oil reservoirs to increase oil recoveries, it can develop first-contact miscibility or multiple-contact miscibility, if the system pressure is higher than minimum miscibility pressure. If the injected CO_2 mix with reservoir oil in all proportions on first contact, it is called first-contact miscibility. With multiple-contact miscible fluids in-situ mass transfer of components occurs between injected and reservoir fluids and all compositions within transition zone of these phases becomes miscible (Stalkup, 1984). But for viscosities 100 to 1000 cp, if CO_2 is not miscible with reservoir oil, the CO_2-EOR can be achieved by swelling oil to sweep the reservoir effectively by decreasing effective mobility

ratio due a large reduction in oil viscosities (Klins, 1984) and thus, immiscible CO_2 can prove to be superior to waterflooding. Due to similar viscosity range of West Sak oil, immiscible CO_2 flooding can be an effective way to increase incremental oil production.

CO_2 injection can be useful in viscous oil reservoirs where thermal methods fail to perform efficiently and CO_2-saturated oil exhibits moderate swelling, in turn reducing oil viscosities and affecting mobility ratio. Klins (1984) enumerates different advantages of injection of CO_2 into oil reservoirs along with its obvious disadvantages. The following are the advantages and disadvantages of the CO_2 injection process for EOR:

Advantages:

i. CO_2 can achieve dynamic miscibility at lower pressure values than methane (Stalkup, 1984)
ii. In the case of CO_2 miscible flooding, the displacement efficiency is high
iii. Overall oil recovery is also increased by solution gas drive
iv. CO_2 injection can be applicable for a wider range of crude oils than other hydrocarbon injection

Disadvantages:

i. CO_2 is expensive to capture from sources and to transport to field locations for EOR

ii. Poor sweep efficiency and gravity segregation are problematic for certain conditions

iii. CO_2 is very corrosive when it is in carbonic acid form

Displacing oil by carbon dioxide injection essentially depends on the number of mechanisms that are inherently linked to the phase behavior of CO_2- oil mixtures (Klins, 1984). Attainment of miscibility or immiscibility during CO_2 injection is a function of reservoir temperature, pressure, and oil composition and hence, the dominant displacement mechanisms fall into one of four following cases:

a) Low pressure scenario
b) Intermediate pressure and high temperature scenario
c) Intermediate pressure and low temperature scenario
d) High pressure scenarios

At pressures below 1,000 psia (case a), the injected CO_2 dissolves in the oil and thereby reduces the viscosity of the oil, swells the oil, contributes to the solution gas drive mechanism, and aids to increase injectivity. Mainly, this low-pressure scenario can be observed in the case of shallow, viscous oil fields.

In case (b), for intermediate pressure (>1000 psia) and high temperature (>122^{o}F) applications, not only the CO_2 injection increases the reservoir pressure and leads to swelling of the oil, but also some of the hydrocarbons may be

vaporized into the gas phase. At the miscible pressure, the oil starts losing its intermediate components into a CO_2-rich gas phase (vaporizing gas drive). Mead-Strawn oil swelled to 40% of its original volume on injection of CO_2 up until 1,400 psia, but above 1,400 psia, the oil phase started shrinking due to hydrocarbon extraction by CO_2-rich phase (Klins, 1984).

For case (c), at intermediate pressure but low temperatures (<122°F), rather than vaporizing oil, CO_2 extracts the lower ends of the oil to form CO_2-rich liquid mixtures. The presence of two liquid phases with (lower pressure) or without (higher pressure) gas phase doesn't prohibit the high oil recoveries. For high-pressure miscible scenario (case d), at pressures of 2,000 to 3,000 psia), injected CO_2 would be able to vaporize significant volumes of oil by generating multiple-contact miscibility in a short period of time and over a very short distance in the reservoir.

Apart from the benefits of immiscible or miscible oil displacement mechanisms by CO_2 flooding, many factors should be considered while designing any CO_2-EOR project (Holm, 1987). Proximity of CO_2 source and available infrastructure may be a limiting factor for many CO_2-EOR flooding projects. Project designers should be wary of the fact that not all the reservoirs can be a candidate for a CO_2-EOR project; reservoir conditions such as temperature, pressure, permeability, and oil saturation and anomalies like fractures can affect the efficiency of the project.

Whether slug injection (and size of slug) of CO_2 followed by water or continuous injection of CO_2 can yield favorable oil recovery is a crucial decision to make and it determines incremental recovery of the project. Adverse mobility ratio of CO_2 injection can also hamper success of an EOR project. As well as the acidic nature of CO_2, in presence of water, should be given due consideration to alleviate the future problems of corrosions in the wells.

Saner & Patton (1983) reported the pilot test of the continuous CO_2 immiscible-drive oil recovery process (due to shallow depth of the Tar zone) conducted in the Wilmington field, Tar zone of the Los Angeles basin. In the early 1960s, primary production from the field was supplemented by waterflooding (secondary recovery). Tertiary oil recovery by immiscible CO_2 flooding was studied in 50-month injection in a large-scale (1,700 acre-ft) pilot. Laboratory experiments were performed to evaluate the process by understanding swelling of the oil-phase and viscosity reduction. It was found that the amount of CO_2 dissolved and in turn an increase in oil swelling, by 105% of original volume, is proportional to increase in pressure. It was observed that the viscosity of the oil was dramatically altered by CO_2 dissolution; viscosity of Tar zone oil was reduced from 283 to 18 cp at a CO_2 pressure of 1,080 psig.

A second series of experiments to test the feasibility of CO_2 flooding involved single-producing well huff 'n' puff stimulation tests. Four tests were conducted

with liquid CO_2 to measure, in situ, the effect of the crude oil/CO_2 interaction on oil and water mobility. The results from these tests showed that each well exhibited strong stimulation in oil production and a large decrease in water production. Initial stimulation ratios were about two to three-fold for oil rates, and a more than ten-fold-magnitude reduction occurred in the flow rate of water.

To increase chances of a successful EOR project, prediction of oil production by reservoir simulation is a way to optimize outcome of a CO_2-EOR project. Reservoir simulation is the most important predictive tool available to the reservoir engineer in comparison with other reservoir production prediction techniques. Black oil and compositional are two reservoir simulation models that are widely used. Black oil models are capable of simulating water, oil and gas phases with negligible dispersion. Phase transfers between the gas and water and the gas and oil are accounted for in the black oil model, whereas compositional model takes the transfer of oil and injection fluid components into account. A simulator based on the compositional model offers an advantage over the black oil model for immiscible or near-miscible displacement when compositionally dependent mechanisms like condensation, vaporization, and oil swelling are essential to understanding when displacement mechanisms are influenced by a compositional dependence of viscosities and densities (Stalkup, 1984). But limitations like i) requirement of a large number of components for accurate prediction of phase behavior, ii) numerical dispersion leading to

erroneous prediction of oil production, and iii) inability to model accurate viscous fingering, observed in CO_2 flooding process, are common to a compositional simulator. In compositional models, it is assumed that the water component is not soluble in the hydrocarbon phase, and the water phase contains only water as a component. This assumption is valid as solubility of water into oil is negligible. But this assumption has a flaw when a significant amount of injected CO_2 dissolves into water.

The flow and pressure equations in either simulation models cannot be solved by the analytical techniques, so numerical solutions are used to solve these equations. The numerical method known as implicit in pressure and explicit in saturation, is used to solve the flow and pressure equations numerically.

Bakshi et al. (1992) carried out a numerical simulation study of CO_2 stimulation process for the West Sak field, using a three-dimensional, three-phase, black-oil simulator. In that study, parameters such as bottom hole pressure, soak period, CO_2 slug size, and the number of cycles were evaluated for the West Sak field. The CO_2 stimulation involved the injection of a slug of CO_2 into the well, followed by a shut-in for several days (soak period). During the soak period, CO_2 travels several hundred feet into the reservoir while displacing mobile water surrounding the well and is absorbed by the oil, reducing its viscosity. After the soak period, the well was allowed to produce. The CO_2 stimulation process can be applicable

to viscous oil reservoirs where absence of miscibility conditions between oil and CO_2 can make the viscous oil reservoir a potential candidate for the stimulation. At the end of a soak period, the region surrounding the well bore area contains mostly low viscosity mobile oil, free CO_2 gas, and immobile water. The maximum oil production rate for a stimulated well was found to be 2.5 to 3 times the maximum oil production rate for unstimulated wells.

Application of immiscible CO_2 injection into the Avile Reservoir, Puesto Hernandez Field, Argentina, was found to be economical, technically feasible and promising (Brush et al., 2000). High permeability and low apparent heterogeneity of the field led to a high sweep efficiency. First, a five-component PR-EOS was developed by a regression technique to match laboratory data, swelling and viscosity data, with the values estimated by tuned EOS. The swelling of oil was 35 percent of its original volume and viscosity reduction by a factor of four by immiscible CO_2 injection. A series of un-steady state CO_2 core flooding experiments were carried out to determine residual oil saturation to waterflooding and to CO_2 flooding with respect to changes in pressure. Furthermore, the core flood tests were simulated with tuned five-component EOS model in a one-dimensional, 180-grid-block model, representing a one-foot composite core. A simulation study predicted oil recovery by CO_2 injection within one percent of laboratory core flood recovery. A pilot area simulation model was generated with log, core, fluid, and production data, spanning 30 years. A black

oil model was used for prediction of production due to primary depletion and waterflooding and then a compositional model was employed to predict oil production during CO_2 flooding.

Klins & Farouq Ali (1981), with a three-phase, two-dimensional simulator conducted a simulation study of immiscible carbon dioxide flooding. It was observed that the oil recovery by carbon dioxide flooding is dependent on initial oil saturation for oil viscosities equal to 100 cp and 1000 cp. For 100 cp oil, recovery increased from 3 to 29% as the oil saturation was increased from 40 to 70%, respectively. CO_2 flooding was found to be superior to other processes such as natural depletion, nitrogen flooding and conventional water flooding for the oil (>70 cp). In the case of 1000 cp oil, the oil recoveries of less than 1%, 16% and 25% were observed for the natural depletion, water flooding, and carbon dioxide flooding, respectively.

Doleschall et al. (1999) performed a simulation study, using a ten-component, three-phase mathematical model, of pure CO_2 and partially miscible carbonated natural gas flooding in the western region of the Budafa oil field, Hungary. Laboratory PVT studies showed that gas containing 81 mole% CO_2 could be used for EOR. At probable optimal CO_2 slug size of 20% pore volume, additional oil recovery was estimated to be 12-16% of the original-oil-in-place.

Prototype reservoir models of a Weyburn unit, which is located in the southeastern part of Saskatchewan, Canada, were developed by Malik and Islam (2000), by using geological and petrophysical data. After successful history matching with previous production data, the models were able to optimize secondary and tertiary recovery schemes. The controlling parameters such as injection in bottom zones and presence of impurities in the CO_2, which influence miscible CO_2 flooding process (tertiary recovery), were studied. Presence of contaminants in the injected CO_2 gas lowered the solubility and diffusivity of CO_2 into reservoir oil, which reduced swelling of oil by CO_2. The low cumulative oil production due to injection of impure CO_2 gas stream into bottom water was attributed to an inefficient transfer of CO_2 from the water phase to the oil phase. Horizontal injection of CO_2 in the reservoir was an effective way to increase anthropogenic CO_2 storage while reaping the benefit of optimized incremental oil production by reducing gravity segregation due to unfavorable mobility ratio.

In another numerical simulation study, Domitrović et al. (2004) planned a tertiary CO_2 injection at Ivanić oil field in Croatia. A numerical model was built with previously acquired seismic data. The black oil model was used to match history of 40 years of production by changing transmissibility of faults. Regression matched PR-EOS along with snapshots of the state of the black oil model initiated compositional model to simulate three different CO_2, and water slug size scenarios. Repressurizing by waterflooding was proved to be important to

increase reservoir pressure to reach to miscibility conditions of CO_2 injection. The incremental oil recovery was more than 88.29 million ft^3 in the scenario with repressurizing of the reservoir.

There are different types of flood pattern that are used for enhanced oil recovery projects. Takur and Sattar (1998) summarized the five-spot, seven-spot, and nine-spot injection patterns for waterflooding projects. Oil companies use similar patterns for CO_2 flooding projects. In the case of a five-spot injection pattern, the typical area of the project is 40 acres. One production well is situated in the center, while four injection wells occupy corners of the square 40-acre area.

2.4 Economic Analysis of CO_2-EOR

Borchiellini et al. (2002) carried out economic analysis and optimization of three existing power plants in Italy by considering effects of CO_2 sequestration vs. carbon tax. In this study, the Environomics technique was used to create the thermoeconomic objective function, in which classic thermoeconomic (i.e. thermodynamics and economics) arguments were extended to include the economic aspect of environmental pollution. Various components of the objective function included: capital cost, cost of the fuel, cost of the CO_2 pollution abatement components, cost of the resources used for the abatement, such as water, limestone and ammonia, and the last term is cost of the pollution of the environment resulting from the cost of operation. Non-linear programming was

used to minimize the objective function to optimize the field of energy system. Since cost of the CO_2 disposal and compression as well as CO_2 tax are difficult to estimate, each of these costs was considered as a parameter. For CO_2 sequestration, a parametric cost analysis based on capital cost was considered in the objective function. This approach is overly complicated as it involves non-linear programming.

Allinson and Ngugyen (2002), as part of the Australian Petroleum Cooperative Research Center's GEODISC project, performed the economic evaluation of CO_2 storage in underground reservoirs by taking into account various uncertainties linked to the costs of storing CO_2. This evaluation, based on the uncertain nature of influencing parameters, was found to be sensitive to the market prices of equipments and services, physical properties of the underground reservoirs, and the CO_2 flow rates. Sensitivity analysis of each parameter was carried out followed by Monte Carlo simulation technique to determine probability distribution of the CO_2 storage costs with respect to the variations in each input parameters. One hypothetical twenty-two year CO_2 storage project example was formulated to illustrate the sensitivity of present value of costs in US$/ton of CO_2 injected to changes in engineering and economic inputs.

Figure 2.1, generated by Monte Carlo analyses, shows the capital cost of CO_2 storage of the hypothetical project could fluctuate between US$ 412 million with

more than 90% confidence and US $734 million with a 10% confidence level and more. The same study for other gases (N_2, CH_4, NO_x, SO_x, and H_2S) showed that storage economics was also a function of composition of the gases that were being stored.

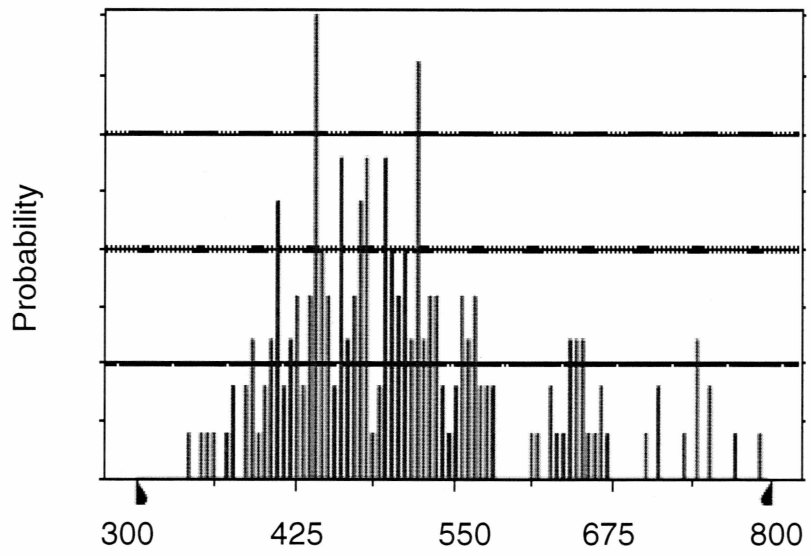

Figure 2.1: Probability distribution of capital cost of CO_2 storage project (Modified after Allinson and Nguyen, 2002)

Transportation cost of any CO_2 pipeline is a useful parameter as this cost will always be part of the CO_2 sequestration project. This cost is mainly influenced by the terrain. For example, a pipeline built on mountainous terrain would be costlier than on the flat terrain. For such conditions the shortest distance analysis method in GIS could assist the project designer to decide which path should be chosen

for gas transport. Removing any water content present in the gas should minimize corrosion of pipelines due to CO_2 and hence reduce operating costs of the transportation. Skovholt (1993) performed a screening study to understand transportation of CO_2 over large distances with a reasonable unit cost. The unit cost of the pipeline could be minimized by properly controlling aspects such as transportation conditions, flow capacity, and pipeline construction methods.

Work by Rubin and Rao (2003) reviewed the key determinates of the CO_2 control cost estimates by defining system boundary, technology, time frame, unreported assumptions to calculate capital cost, and operating costs of carbon capture and storage (CCS) project. Assumptions for the capacity factor of the capture plant and efficiency of the power plant should be transparent to avoid any misunderstanding of the CCS economics. Furthermore, in a case study of new pulverized plant with amine based CO_2 capture unit, Rubin and Rao (2003) illustrated the effect of the uncertainties on CO_2 control cost by using a computer model, developed by the U.S. Department of Energy.

Senior et al. (2004) analyzed the capital investment requirements for a large-scale CCS project along with the emission reductions to evaluate when and how CCS should be deployed in the power sector. The authors overviewed costs and cost drivers for capture, transportation and storage, as given in Table 2.1, which could act as the basis for any CCS project.

Table 2.1: Overview of CCS project costs and cost drivers (Modified after Senior et al., 2001)

Segment	Costs, $/ton of CO_2	Common Cost Drivers	Specific Cost Drivers
Capture	5-90	Volume of CO_2 Location Onshore/Offshore	Type of Sources Retrofit
Transportation	0-20		Distance from sink Existing infrastructure Ship vs. pipeline
Storage	2-12		Existing infrastructure Size of storage field Monitoring requirements

Similarly, Pike (2006) provided the cost of carbon sequestration project with or without CO_2 capture for geological storage and EOR projects for natural gas combined cycle, pulverized coal type, and integrated gasification combined type of Power plants. For natural gas combined power plant with geological storage, US$ 0.04-0.08 per kilowatt-hour of energy produced would be the cost of CCS, while US$ 0.04-0.07 would be the cost of CCS combined with EOR. The CCS costs were the highest for pulverized coal type power plant. Thus, selection of type of new power plant, closer to the deemed sequestration site, is important for any future CCS projects.

In 1991, British Coal began a program to develop fossil fuelled power generation and integral CO_2 removal and disposal. In this study, a range of different options, such as: CO_2 disposal options; options for power plants; CO_2 separation process and disposal route options, were studied. Summerfield et al. (1993) was able to show that the cost of CO_2 disposal contributed a large portion of the cost of a low CO_2 generation system. The cost of CO_2 transport and removal ranged from around £18-£108 per ton (US $33-203/ ton) of CO_2 emission avoided, depending on the type of power plant, and the CO_2 separation and disposal options.

Price of oil always determines the present value of any CCS project with EOR. Morgan (2005) performed stochastic modeling as a prediction of future Canadian oil prices. It has inherent flaws due to its dependency on fluctuating supply and demand. In the stochastic model, changes in oil price are set as a function of difference between the current spot price and mean-reversion price, reversion rate, and price volatility. Such stochastic modeling of oil prices is essential to predict the future trend of oil price fluctuation, which is essential for decision makers to decide fate of a CO_2-EOR project. Similar studies in the future could be useful to understand fluctuation in oil prices in the US.

Net present value (NPV) is considered as the most accepted economic index in the oil industry. Cash flows, lifetime of the project, and time value of the money are included in the calculation of NPV. NPV is a measure of profit and thus it

yields the direct measure of the success of the project. To determine economic feasibility, a study based on the NPV and sensitivity analysis of the CO_2-EOR project in a small mature Brazilian oil field was carried out by Gasper et al. (2005). NPV of the project was calculated by taking into account the capital expenditures, operating expenditures, price of oil, CO_2 credits, taxes, and the capture, transport, and storage costs of the CO_2 injection in a cash flow model. Initial investment arising from the capture from fertilizer plant, compression, and storage and transport of CO_2 gas was included as capital expenditure of the project. NPV of the project, at a discount rate of 12%, was calculated to be $3.2 million, which is significant for the small field.

On the other hand, GIS based carbon management can also be used to select economically feasible EOR projects. One such study by Dahowski et al. (2001) developed a GIS-based carbon management strategy to economically screen oil reservoirs amendable to EOR.

Though the United States does not provide incentives like CO_2 credits to the industries for abatement of CO_2 emissions, in the near future, introduction of such CO_2 credits is highly possible due to increased public concern to global warming. Once such credits are started for CO_2 abatement, net carbon flow calculations must be performed to deduct the amount of sequestered CO_2 that otherwise would be released into the atmosphere.

2.5 CO_2 Sequestration in Saline Aquifer

Thick, highly permeable and porous saline aquifers with impermeable cap rock are the ideal formation target for CO_2 sequestration. Deep and laterally extensive aquifer formations are essential for the slow flow of CO_2 gas bubbles to the top of the formation. Injected CO_2 is always less dense than the saline formation water and may migrate to the top of the formation (Benson, 2003).

The mineralogy of aquifer formation rock dictates the geochemical binding of the CO_2 molecule to rock mineral in the form of various carbonates (Prucess et al., 2003 and Sass et al., 1998). Predominately, the injected CO_2 occupies the free gaseous phase in the available pore space and some fraction of CO_2 dissolves into water. Solubility of CO_2 takes place according to Henry's law, which is a relation between partial pressure of the dissolving gas and its concentration in the aqueous form. Increase in temperature and salinity of water decreases the solubility of gases in the aqueous phase, while increase in pressure of the system increases solubility of gas in the water.

Whether the injected CO_2 is found in liquid, gas, or a supercritical fluid state depends on the pressure and temperature. The effect of pressure, at 45°C, on density and viscosity of a CO_2 + water system is given in Table 2.2 (Oostrom et al., 2003). At 2352 psia, the density of the supercritical CO_2 (critical temperature of 31.1°C and critical pressure of 1071.63 psia) is higher than that of 1764 psia. It

is worth noting that the difference between the density of pure water and CO_2 gas decreases from 336.2 kg/m^3 at 1764 psia to 235.4 kg/m^3 at 2352 psia, which is important to reduce the buoyancy effect due to the large density difference.

Table 2.2: CO_2 and water properties at 45° C (Modified after Oostrom et al., 2003)

Fluid Phase		1764 psia	2352 psia
Pure water	Density (kg/m^3)	994.768	996.292
	Viscosity (Pa s)	5.9778×10^{-4}	5.98341×10^{-4}
Water with CO_2	Density (kg/m^3)	994.768	996.292
	Viscosity (Pa s)	5.9778×10^{-4}	5.98341×10^{-4}
	CO_2 mass fraction	5.22541×10^{-2}	5.70921×10^{-2}
Gas	Density (kg/m^3)	658.574	760.891
	Viscosity (Pa s)	5.16820×10^{-5}	6.56320×10^{-5}
	Water mass fraction	9.93985×10^{-5}	8.60323×10^{-5}

Van der Meer (1996) studied commercial capabilities of reservoir simulators based on the Darcy flow, to predict the effects of CO_2 injection in an aquifer by comparing the results with previous studies based on the user-defined equilibrium ratio value and gas solution ratio approach. The author used the Gas-Water option of the SIMBEST II SSI simulator for this study. It was observed that local grid refinements, displacement front tracking methods and inclusion of a function to describe dependency of solubility on time and salt concentration could improve simulation results.

Shan and Pruess (2004) developed an improved model over TOUGH2's previous model, in which Henry's law and gas diffusivity coefficients were considered constant, by introducing temperature dependence of the coefficients. The importance of this study is the inclusion of temperature dependent diffusivity and Henry's law constant terms, which many of the gas displacement algorithms don't incorporate in their codes. This thermodynamic reliance of the coefficients is useful when there are significant variations in temperature and pressure. But it should not be used when temperature is in the range of 10-20°C, for example ground water problems. The new model can be used to study CO_2 sequestration in saline aquifers where temperature and pressure of the system vary due to the injection of CO_2.

Prucess et al. (2003), at Lawrence Berkeley National Laboratory, carried out an in-detail numerical modeling study of disposal of CO_2 into brackish (saline) aquifers. At the beginning of their study, the sequestration capacities using volumetric estimates were calculated. Then the numerical simulation showed the effect of gravity overriding because of bypassing of water by the CO_2-rich gas-like phase. The gravity overriding phenomenon due to the density difference between the water and gas phase led to increase in gas saturation in the vertical direction, thus decreasing the contact volume of aquifer by CO_2 gas. For the thirty-year injection of CO_2 gas in the aquifer, a CO_2 plume of an approximately 38.61 $mile^2$ area and the aquifer pressure increased by 14.7 psia over the area of

956.26 mile^2. Changes in morphology of the rock matrix and reduction in porosity due to the formation of secondary carbonates is also an important factor and must be included in designing any numerical code.

A mathematical model for the CO_2 displacement studies is a set of differential equations for each grid cell, describing the conservation of mass and the superficial velocity for water, gas and oil, if present. To study simulation of CO_2 displacement and long-term storage in underground formation in general, deep saline aquifers in particular, require algorithms with multi-fluid capabilities to predict phase transitions (Oostrom et al., 2003). Modeling of CO_2 dissolution in saline aquifers should be able to take into account buoyancy driven flow due to density difference, Rayleigh instability fingering arising from viscosities of displacing and displaced phases, aqueous dissolution, molecular diffusion, hydrodynamic dispersion, and phase transitions.

In a study by Saripalli et al. (2003), a semi-analytical model to simulate sequestration of CO_2 in deep geological formations was developed. Since phase behavioral properties (for example density) do not change drastically with changes in temperature, isothermal conditions were assumed in the semi-analytical model. It was concluded that the semi-analytical model could effectively simulate injection of water-immiscible, gaseous, or supercritical carbon dioxide into confined formations. However, semi-analytical model assumptions

such as uniform formation properties and instantaneous dissolution of CO_2 in the formation water are not real life situations. Laminar flow (low Reynold's number) of the formation water can slow the dissolution of CO_2, making the dissolution process rate limiting in the sequestration. Pacific Northwest National Laboratory's (PNNL) Subsurface Transport Over Multiple Phases (STOMP®)-*Water-CO_2-NaCl* (WCS) numerical model is an advanced numerical model used to simulate the dissolution non-equilibrium adequately. STOMP®-WCS can simulate changes in hydrological properties, especially the porosity and relative permeability. But temperature changes in geothermal gradient of the formation due to injection of supercritical CO_2, which is necessary in the permafrost regions of the Alaskan North Slope, are needed to simulate and to observe increase in temperature, if there is any. By including energy equations in *Water-NaCl-CO_2* operational mode of the STOMP®, another simulator model, represented as *Water-CO_2-NaCl-Energy* (WCSE), was generated by PNNL. In the present study, STOMP®-WSCE was used to simulate sequestration of CO_2 in a deep saline aquifer.

Chapter 3

Methodology

3.1 Alaskan North Slope Oil Pools: Parametric Screening

The ranking of the oil reservoirs to evaluate the technical feasibility with respect to their CO_2-EOR potential was performed by calculating the rank of the reservoirs for EOR studies by comparing the parameters like oil gravity (^{o}API), porosity (Φ), permeability (k), temperature (T), pay zone thickness (h), oil saturation (S_o), and MMP with the optimum reservoir parameters (Table 3.1). All the parameters but MMP were obtained from the oil pool database of Alaska Oil and Gas Conservation Commission (2003). The detailed step-wise procedure for ranking is discussed below:

a) Estimation of MMP

The calculations of MMP for oil and a pure CO_2 system rely on the proper characterization of oil, particularly the C_{5+} component. To circumvent the tedious and time-consuming nature of collecting oil composition for each oil pool on the ANS, a simpler method reported by National Petroleum Council (Ahmed, 1997) to predict MMP, based on API gravity and temperature of the system, was used in this study. Based on this method, for API gravity less than 27, MMP is 4000 psia and as the API gravity increases MMP is found to decrease with a reservoir temperature correction. The description of this method can be obtained from the work of Ahmed (1997).

b) Normalization of parameter

Normalized parameter ($X_{i,j}$) is given by,

$$X_{i,j} = \frac{\left| P_{i,j} - P_{o,j} \right|}{\left| P_{w,j} - P_{o,j} \right|} \tag{3.1}$$

Where $P_{o,j}$ is the magnitude of parameter (j) in an optimum reservoir, which results in optimum CO_2 flooding. These optimum parameters were obtained from the studies by Rivas et al. (1992). The optimum properties of the optimum reservoir were determined by performing a numerical simulation, which optimized the reservoir response to the gas flooding. $P_{w,j}$ is the magnitude of the parameter of a worst reservoir for CO_2-EOR, which was determined from the data bank of the reservoirs to be screened. For each reservoir parameter, the value farthest from the optimum value was then selected as the worst value of that parameter. $P_{i,j}$ is a parameter into consideration for the i^{th} reservoir.

c) Transformation to exponential function

Since exponential function is more adequate than linear function for comparing different elements in same set, $X_{i,j}$ was transformed into an exponentially varying function ($A_{i,j}$) as given below:

$$A_{i,j} = 100 \times e^{(-4.6X^2_{i,j})} \tag{3.2}$$

d) Generation of weighted grading Matrix

To account for the relative importance of each reservoir parameter, a weighted grading matrix, $W_{i,j}$ is determined as follows:

$$W_{i,j} = A_{i,j} \times w_j \tag{3.3}$$

Where w_j is the weight of each reservoir parameter. Table 3.1 gives optimum values with respective weights assigned to each parameter, while worst values for each parameter for oil pools on ANS are given in Table 3.2.

e) Rank of the reservoir (R_i)

Ranking of the reservoir is given as:

$$R_i = 100 \times \frac{\sum_{j=1}^{j} M_{i,j}}{\sum_{j=1}^{j} M_{1,j}} \tag{3.4}$$

Where $M_{i,j}$ is the product of $W_{i,j}$ and its transpose $W_{j,i}$. $M_{1,j}$ stands for the values corresponding to the optimum reservoir.

Table 3.1: Optimum reservoir parameters with respective weights (Modified after Rivas et al., 1992)

Parameter	Optimum	Weight
API Gravity	37	0.24
Oil saturation, %	60	0.2
Pressure/ MMP	1.3	0.19
Temperature, °F	160	0.14
Net thickness, ft	50	0.11
Permeability, md	300	0.07
Porosity, %	20	0.02

Table 3.2: Worst parameters from ANS oil pool database

Parameter	Upper Limit	Lower Limit
API Gravity	44	17.5
Oil saturation, %	90	50
Pressure/ MMP	4.11	0.4
Temperature, °F	254	75
Net thickness, ft	290	20
Permeability, md	1007.5	1.5
Porosity, %	30	10

3.2 Characterization of West Sak Oil and Phase Behavior with CO_2

Live West Sak oil is characterized by 23 components (Table 3.3) with the molecular weight of a heavy component (C_{21+}) as 455 lb/lbmole (Bhandari, 1988). Experimental data on constant composition expansion and differential liberation experiments on the West Sak oil provided the values of relative oil volume, percentage liquid volume, oil viscosity, gas oil ratio, and specific gravity of gas at different pressures, as reported by Roper (1989). A compositional PVT simulator (WinProp®), developed by Computer Modeling Group (CMG), was used for this study. It minimizes the sum of squares of the relative errors by using regression technique for PR-EOS (1978) tuning, and calculates the values of different properties before and after EOS tuning. Furthermore, C_{7+} components of the West Sak oil were regrouped into five components by the equality of mole fractions method to save the time required for the compositional simulation study. Tuning of regression parameter was carried out by setting up variables such as critical properties and acentric factors of components C_7 through C_{21+}. In addition to that, omega A and B parameters for methane and C_{21+}, viscosity parameters, and interaction coefficients were used as regression variables (Danesh, 1998). The step-by-step procedure of lumping of components and tuning of EOS is given in Appendix A. Tuned EOS was implemented in the compositional simulation study of CO_2 injection for enhanced oil recovery.

For simplicity, the ternary phase behavior diagram can be defined as a representation of 3 different components at constant pressure and temperature. Pseudo-ternary diagrams are used for multi-component mixtures by combining several components into three groups, representing three apexes on the ternary diagrams. Tuned PR-EOS (1978) was then used as the new EOS for West Sak oil and 100% CO_2 system. The PVT simulation of CO_2 injection into the oil was carried out to generate pseudo-ternary diagrams. It resulted into formation of two different phases from the mixture. The initial pressure of 1600 psia was increased in a step-wise manner to observe the miscibility condition for West Sak oil and CO_2.

Table 3.3: West Sak oil composition (After Bhandari, 1988)

Component	Mole Percent	Component	Mole Percent
CO_2	0.016	C_{11}	1.72
N_2	0.032	C_{12}	1.346
C_1	38.333	C_{13}	1.496
C_2	0.857	C_{14}	1.795
C_3	0.359	C_{15}	1.944
C_4	0.179	C_{16}	1.795
C_5	0.064	C_{17}	1.57
C_6	0.2	C_{18}	1.795
C_7	0.016	C_{19}	2.468
C_8	0.008	C_{20}	2.841
C_9	0.823	C_{21+}	39.037
C_{10}	1.496		

3.3 Simulation of CO_2 Injection for Enhanced West Sak Oil Recovery

Generalized Equation-of-State Model (GEM®), developed by the Computer Modeling Group, is an efficient and multidimensional compositional simulator. This simulator was used to conduct CO_2 displacement studies by taking into account gas injection processes like vaporization and swelling of oil, condensation of gas, viscosity and interfacial tension reduction, and solubility of CO_2 in water.

The Explicit mode for solving forward-difference formulation, which evaluates inter-block-flow equations, suffers from restrictions on the time-step size due to conditional stability of the procedure. But GEM's adaptive implicit formulation by using implicit formulation (unconditional stability is achieved but it is time consuming) of the flow equation chooses, at every time-step, which grid blocks should be solved either in implicit mode or explicit mode and thus saves time required for a simulation run. The adaptive implicit mode for applications involving high flow rates (at injection wells), pressure gradients near wells, and for flow through very thin layers (in the case of West Sak reservoir) is beneficial.

3.3.1 Grid System and Petrophysical Properties

A three-dimensional Cartesian grid system was adopted for this study. A total of 5625 grid blocks were divided as 25, 25, and 9 grids in X, Y, and Z direction (Figure 3.1), respectively. Due to the vast nature of the West Sak reservoir, a

five-spot injection pattern (40 acres) was considered in the current simulation work. The distance between the adjacent injection wells was 1320 ft and that of between the injection and production well was 933 ft. All injection wells were on the corners of the square area while the production well was set in the center, at the midpoint of bisectors. Figure 3.2 shows the 40-acre pattern. Continuous CO_2 was injected for 25 years in the injection wells so that the total injected CO_2 was 10%, 20%, 30%, and 50% of the pore volume (PV) of reservoir.

Each porous and permeable bed was considered as one layer of productive sand with average porosity, thickness, and water saturation. Shale layer, which acts as an impermeable layer (inactive) with zero porosity, separated the sand layers. The average values of the important petrophysical properties for the five sand layers are given in Table 3.4. During production and injection, reduction in internal pressure can lead to decrease in porosity, especially above bubble point pressure. A constant rock compressibility of 5×10^{-6} per psi was assumed for this simulation study (Bakshi, 1991).

Table 3.4: Average layer properties of West Sak for 40-acre injection pattern (After Bakshi et al., 1991)

Layer No.	Sand	Interval (ft)	Avg. Porosity (%)	Avg. water saturation, (%)	Net pay (ft)
9-topmost	Upper 1	3544-3584	30	24	30
7	Upper 2	3614-3640	31	31	21
5	Lower1	3660-3686	23	45	3
3	Lower2	3695-3760	25	47	3
1-bottommost	Lower3	3776-3814	27	41	17

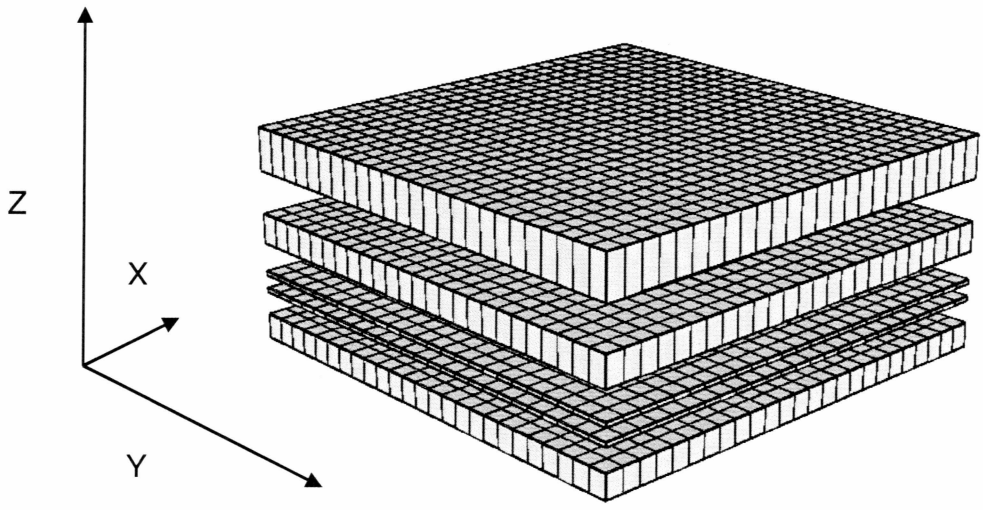

Figure 3.1: Three-dimensional view of the grid system

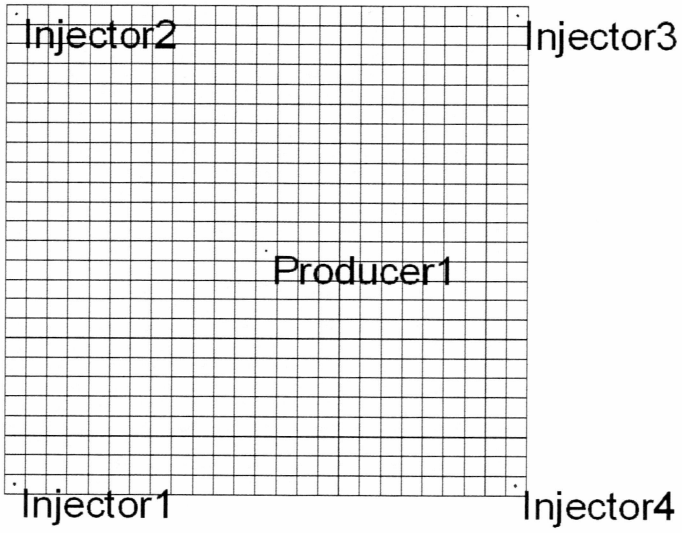

Figure 3.2: Five-spot CO_2 injection pattern

3.3.2 Relative Permeability Data

From a previous study by Bakshi (1991), the water-oil relative permeability and gas-oil relative permeability data was acquired. A West Sak operator had provided the data on the relative permeability. The water-oil relative permeability curves for the West Sak Upper Sand #1, Upper Sand #2 and Lower sands are given in Figures 3.3 3.4, and 3.5, respectively. While, Figures 3.6, 3.7 and 3.8 are the graphical representation of the gas-oil relative permeability for the Upper Sand #1, Upper Sand #2 and Lower sands, respectively. These relative permeability (K) curves were digitized for use in this simulation study. The subscripts 'o', 'w' and 'g' represent oil, water and gas phases, respectively.

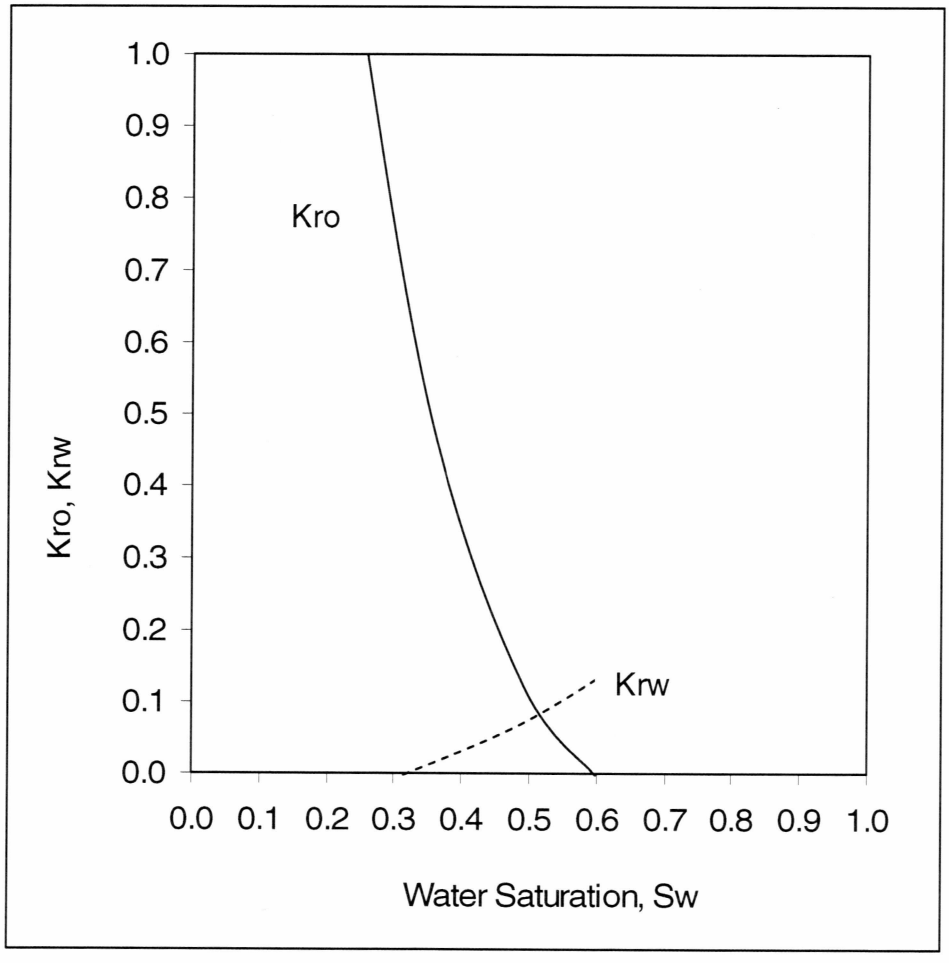

Figure 3.3: Water-oil relative permeability of West Sak upper sand #1 (Modified after Bakshi, 1991)

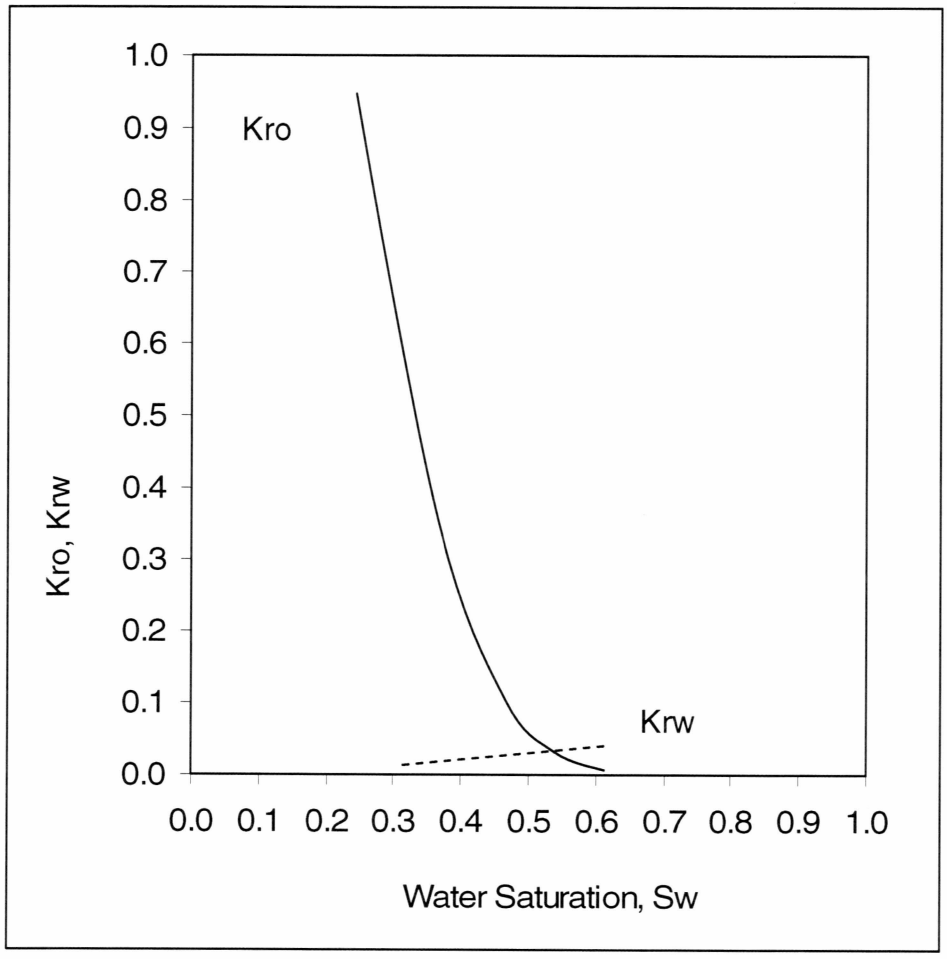

Figure 3.4: Water-oil relative permeability of West Sak upper sand #2 (Modified after Bakshi, 1991)

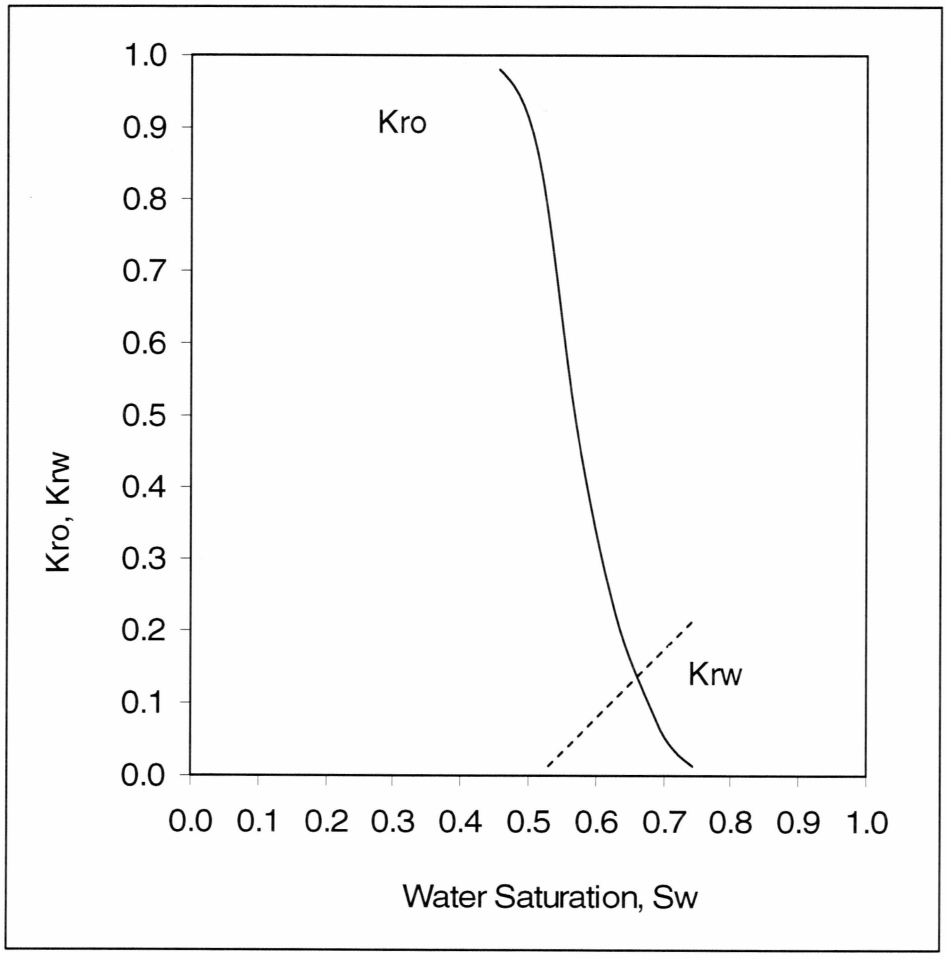

Figure 3.5: Water-oil relative permeability of West Sak lower sands (Modified after Bakshi, 1991)

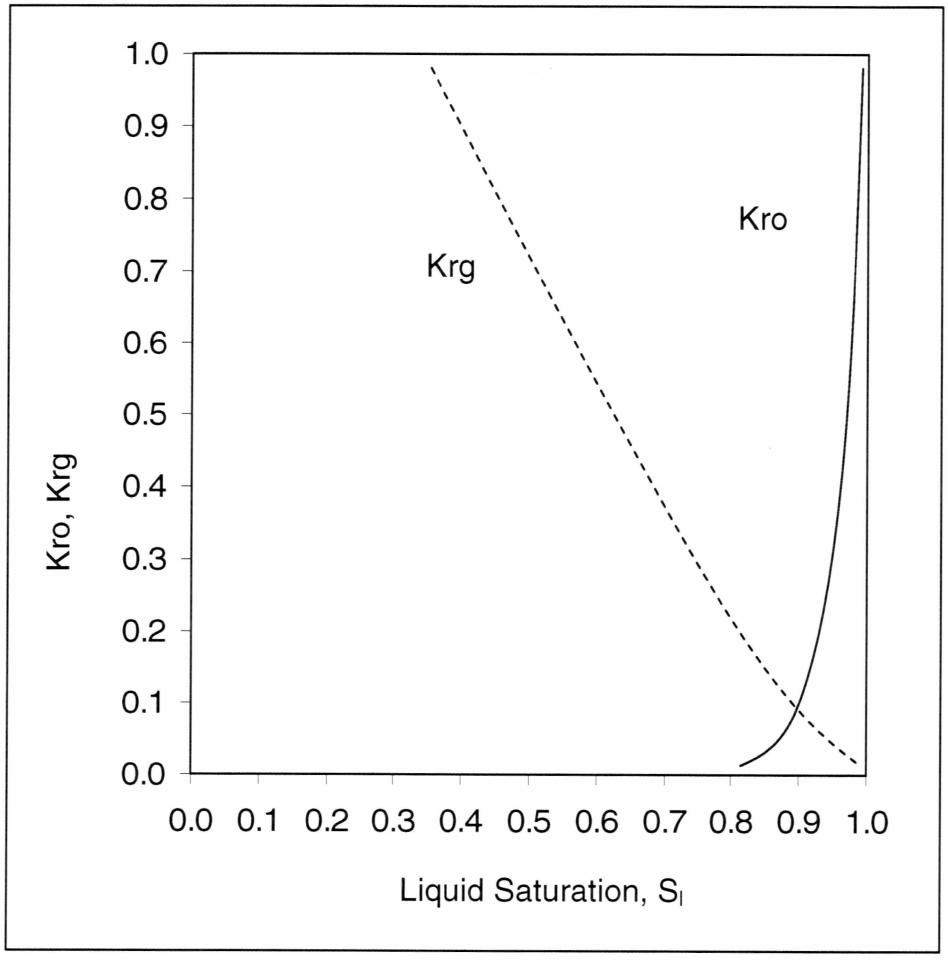

Figure 3.6: Gas-oil relative permeability of West Sak upper sand #1 (Modified after Bakshi, 1991)

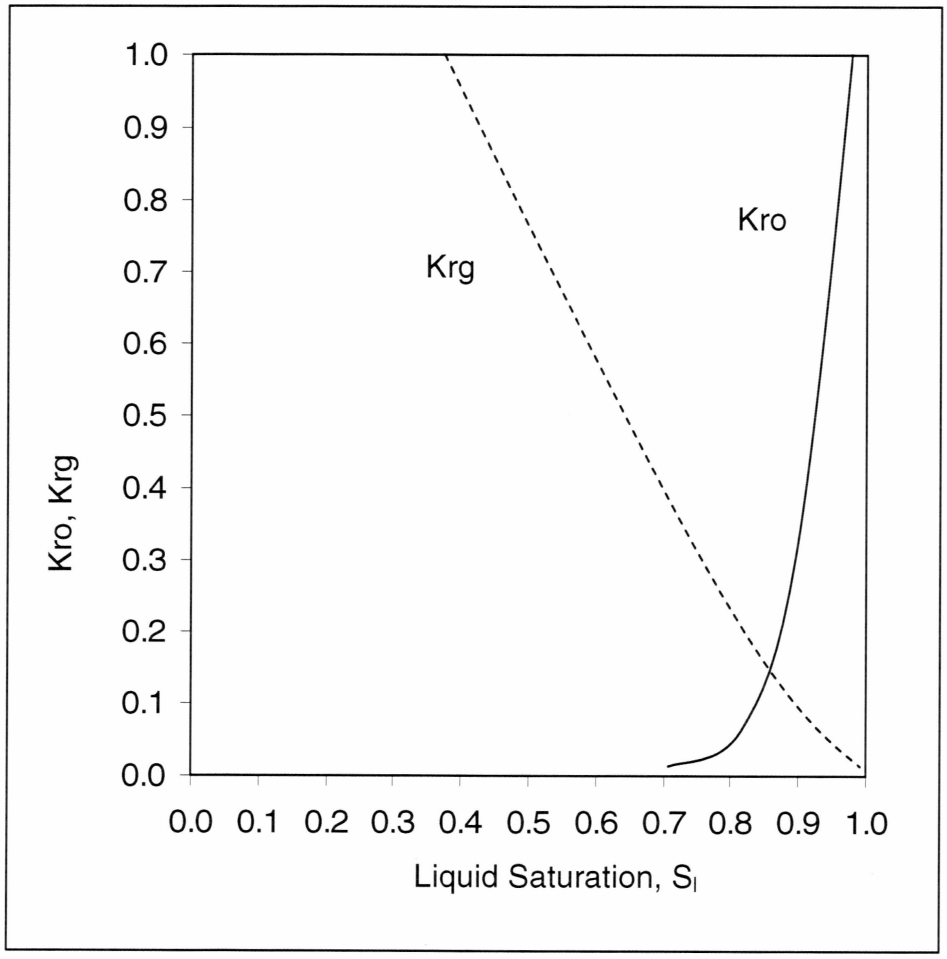

Figure 3.7: Gas-oil relative permeability of West Sak upper sand #2 (Modified after Bakshi, 1991)

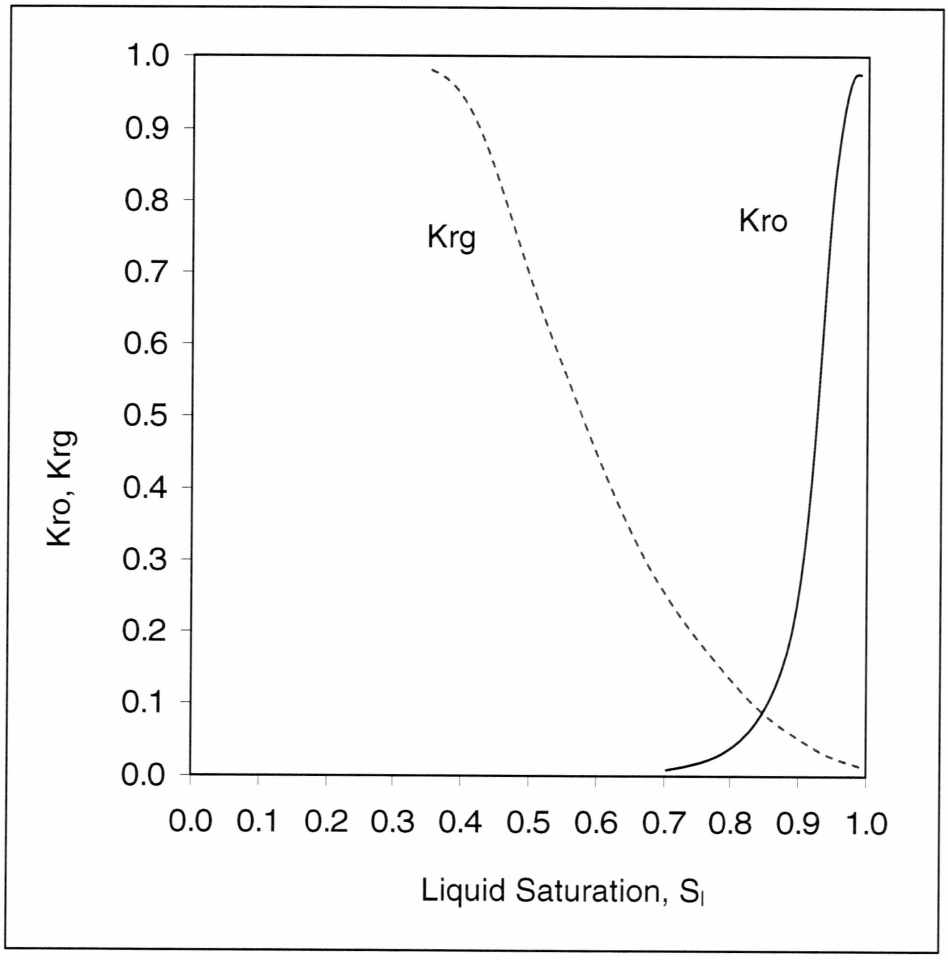

Figure 3.8: Gas-oil relative permeability of West Sak lower sands (Modified after Bakshi, 1991)

3.4 Economic Feasibility of CO_2 Sequestration with EOR

In this part of the study, an economical analysis of the CO_2-EOR project was carried out to evaluate the feasibility of CO_2 sequestration with EOR. A cost for each stage of CO_2-EOR project includes:

a. Capital Expenditures (CAPEX) that include initial investments for transportation, capture, compression, and storage of CO_2

b. Operating Expenditures (OPEX), which include labor and maintenance costs for transportation, capture, compression, and storage of CO_2

Apart from the CAPEX and OPEX, the economics of the CO_2-EOR project is also influenced by market prices of equipment and services, life of the project, fiscal regime, price of the oil, and all the sundry costs related to the recompletion of wells and drilling. According to Gasper et al (2005), the annual net cash flow (NCF) of CO_2-EOR project can be calculated as follows:

NCF= [Gross revenue from oil production + CO_2 credits – Royalty – OPEX - Annual drilling or completion cost (if any) - Rental cost - Depreciation] × (1 - Corporate tax) + Depreciation - CAPEX (3.5)

In equation 3.5, the gross revenue is the product of oil price and production rates. The credits of CO_2 are incorporated as an additional gain by keeping in mind that

the implementation of CO_2 credits in the future is inevitable by providing incentives to the industries for reducing CO_2 emission by sequestration.

Using simulation results obtained from the 40-acre injection pattern of West Sak oil by 50% PV of CO_2 injection and multiplying the area by 75 (3000 acres) to justify the initial investment in carbon dioxide capture, compression, transportation, and storage. It was assumed that there were 75 five-spot injection patterns. The NPV of the 3000 acres CO_2-EOR project was calculated from the following assumptions, based on the study of Brazilian oil fields. Hence, assumptions were according to the Brazilian fiscal regime, by Gasper et al (2005), as illustrated in Table 3.5. The values of corporate tax, royalty, and rent were changed as per the Alaskan fiscal regime. CO_2 credits in equation 3.5 was determined by multiplying total injected CO_2 with credit per ton of CO_2 and storage ratio, values of which were assumed to be US $10/ton and 0.38, respectively. The storage ratio was calculated as given in equation 3.6:

$$\text{Storage Ratio} = \frac{\text{Quantity of } CO_2 \text{ stored}}{\text{Total quantity of } CO_2 \text{ injected}} \tag{3.6}$$

To investigate the impact of variables such as oil price, discount rate, OPEX costs, and CO_2 credits on NPV, sensitivity analysis was performed. Values of variables and assumed distribution are given in Table 3.6. Additionally, the Monte

Carlo simulation technique in Crystal ball® software was used to show the probability distribution of NPV by overcoming problems associated with a limited range of input variables. The Monte Carlo simulation technique randomly generates values for uncertain variables over and over to simulate a model and thus considers full range of uncertainty for a variable.

Table 3.5: Assumed values of parameters for net present value calculation

Parameter	Assumed Value for NPV
Oil Price (US $/bbl)	50
Project Life (years)	25
Royalty	12.50%
Corporate Tax	35%
Discount Rate	12%
Rent	$12/acre
Storage Ratio	38 %
CO_2 Credits (US $/ton CO_2)	10
Capture Cost (US $/ton CO_2)	3
Compression Cost (US $/ton$CO_2$)	7.5
Transportation Cost (US $/ton CO_2)	8
Storage Cost (US $/ton CO_2)	3

Table 3.6: Assumed distribution and parameter values of variables for sensitivity analysis

Variable	Distribution	Parameter Values
Discount Rate	lognormal	mean = 12%; standard deviation = 4%
Oil Price	lognormal	mean = 50; standard deviation =10
CO_2 Credits	lognormal	Mean =10;standard deviation = 5
Storage Cost	triangular	1.5; 3; 4.5
Capture Cost	triangular	1.5; 3; 4.5
Compression Cost	triangular	6; 7.5; 9
Storage ratio	normal	mean = 38%; standard deviation = 10%
Transportation Cost	triangular	6; 8; 10

3.5 CO_2 Sequestration in Saline Aquifer using STOMP®-WCSE

Advantages of injection of supercritical CO_2 (2352 psia and 45°C) are discussed in Chapter 2. However, injection of supercritical CO_2 in the saline aquifer could be detrimental to permafrost region, when injected heat travels through the formation by conduction or convection and can increase temperature in the permafrost region. To alleviate this problem, deep saline aquifers with low vertical permeability should be chosen for CO_2 injection in order to minimize any heat conduction due to fluid movement.

A 2-D cylindrical model (42 grids in horizontal direction and 28 grids in vertical direction) was formulated for STOMP®-WCSE simulation runs. Figure 3.9 illustrates the 2-D model, representing four different layers. Total depth of the

formation was 4780 ft from the top and the model spans 5280 ft (1 mile) horizontally. According to STOMP®, S user guide (White and Oostrom, 2003), an input file was written to include, for example, relative permeability functions, thermal properties of the formation, and permeability and porosity values of each layer. Injection of 4.40 lb/sec of supercritical CO_2 in layer #1, having porosity of 30% and a constant permeability value of 1 darcy in horizontal and vertical direction was simulated. The injection well was assumed to be perforated 100 ft in the layer #1. Permeability of layers 2 and 3 was 1×10^{-6} and 0.1 darcy, respectively. At the beginning of simulation, the pressure and the temperature in the bottommost grid were 2055 psia and 39°C, respectively. The geothermal gradient of 0.0127°C/ft was set for layers 1, 2, 3 and water body, while permafrost gradient was set to 0.0015°C/ft. The geothermal gradients were calculated so that the temperature at the bottom of the permafrost region was 4°C and the top was 0°C. Sodium chloride mass fraction for layers 1, 2 and 3 was assumed to be 0.05, while that for permafrost and water body was set to zero. At the rate of 4.40 lb/sec, total of 1.39×10^9 lb of CO_2 was injected in the ten-year injection period; changes in CO_2 gas saturation, its aqueous mass fraction, and temperature profile were observed for 20 years.

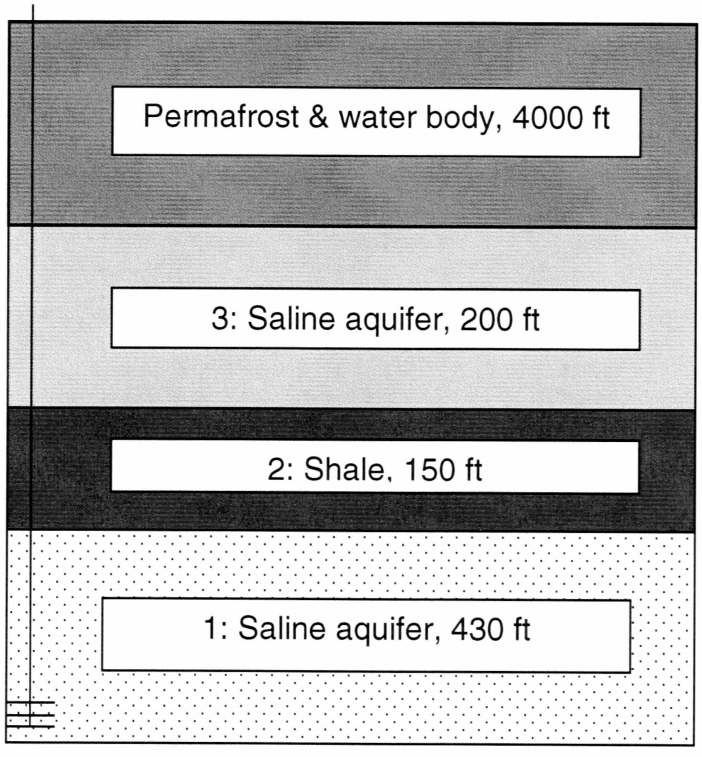

Figure 3.9: 2-D cylindrical model used in STOMP®-WCSE

Chapter 4

Results and Discussion

4.3 Ranking of ANS Oil Pools Based on Screening Criteria

The screening of ANS oil pools with the parametric approach, which is based on the optimum parameters and assigned weights to each parameter, has the advantage of selecting potential pools for CO_2-EOR. The values of gravity of various oils from ANS-oil database mostly delineate the suitability of an oil pool for CO_2-EOR. Table 4.1 lists the petrophysical properties of a few ANS oil pools, while the last column gives the rank of oil pools, according to the study by Rivas et al. (1992). From Table 4.1 shows the screening of fourteen of the ANS oil pools. The oil pools with high ranks have low amenability with respect to EOR. It is evident that oil pools with lower gravity (viscous oil) have been placed lower in the ranks, while this is not entirely true for the light-oil (higher API gravity); Ivishak pool, which would be last pool to get chosen if such selection of ANS oil pools were performed. This explains how parameters other than gravity play a role in screening; in the case of low porosity of 15% for the Ivishak pool has hampered its suitability. West Sak pool with the rank of 11 has been selected for future phase behavior and simulation studies for CO_2 flooding due to the economical inapplicability of a conventional enhanced oil recovery processes like water flooding to produce from abundant West Sak oil.

Table 4.1: Parametric ranking of oil pools on ANS with respect to optimum reservoir parameters

Pool	T,°F	Φ, %	k, md	S_o, %	h, ft	°API	P/ MMP	R_i
Pt. Mcintyre	180	22	200	60	156	27	1.27	1
Meltwater	140	20	10	60	95	36	1.5	2
Lisburne	183	10	1.5	70	125	27	1.03	3
Tarn	142	20	9	60	40	37	1.64	4
Prudhoe	200	22	265	70	222	28	0.94	5
Alpine	160	19	15	80	48	40	1.81	6
Kupurak -Milne	160	20	150	90	100	24	0.79	7
Kupurak River	165	23	40	70	35	22	0.76	8
Sag River	234	18	4	60	30	37	1.86	9
North Prudhoe	206	20	590	60	20	35	2.07	10
West Sak	75	30	1007	70	70	19	0.41	11
Schrader Bluff	80	28	505	70	70	17.5	0.4	12
Hemlock	180	10.5	53	70	290	33.1	2.34	13
Ivishak	254	15	200	50	125	44	4.11	14

4.2 Phase Behavior of West Sak Oil with CO_2

The performance of untuned and tuned PR-EOS for prediction of percentage of liquid volume and relative oil volume are shown in Figures 4.1 and 4.2, respectively. Clearly, these figures demonstrate the importance of the tuning process, which would help in reliably predicting the phase behavior of the West Sak oil under CO_2 injection at various pressures values.

In pseudo-ternary diagrams (Figure 4.3), CO_2 was lumped with the intermediate components (C_2-C_6) to form an intermediate fraction. At lower pressures, closer to West Sak reservoir pressure, the vapor phase consists of intermediate and light components (Figure 3: a). At the lower pressure, partial miscibility of CO_2 with West Sak oil fluid is present. As the pressure of the system increases, the heavy and light components were found to be present in either vapor or liquid phase, while the intermediate components were present, mainly, in the vapor phase (Figure 4.3: b). At a pressure of 3600 psia and more, the nature of shrinking ternary plots remained unchanged, which was contrary to most of the miscibility conditions, observed in the vaporizing or condensing drive. In the case of CO_2 injection, vaporizing of intermediate oil components by CO_2 is a dominant displacement drive mechanism. So as to represent the vaporizing drive on the ternary diagram, the tie line at a critical point should pass through the reservoir fluid. But this phenomenon was clearly absent in the diagrams at higher pressures, as can be seen in Figure 4.3. In the description of displacement

mechanisms by Zick (1986) and Stalkup (1987), it was observed that a combination of condensing and vaporizing drive led to displacement of the oil in the case of enriched gas injection. By applying the same logic in this study, for CO_2 injection at a pressure of 3600 psia and higher, as injected CO_2 came into contact with the West Sak oil, the intermediate components were vaporized into CO_2 gas, which resulted in a richer injection gas. As this heavier gas moved further into fresh oil, its capacity to vaporize intermediate components would diminish after few contacts. Lighter fractions of the intermediate components from heavier injection gas started condensing into oil, which resembles to the condensing mechanism of enriched gas injection. Hence the combination of vaporizing and condensing mechanisms was observed in this study. The gas in the vaporizing/condensing mechanism never becomes rich enough to be miscible with the original oil. This apparent miscibility can explain the nature of ternary plots, wherein injected gas and oil are apparently miscible but not miscible.

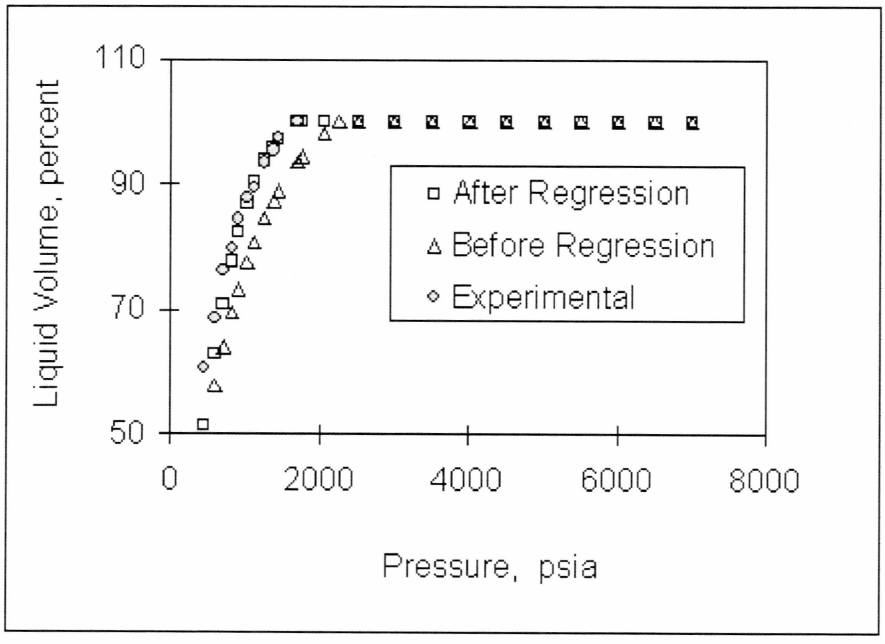

Figure 4.1: Percentage of liquid volume before and after regression

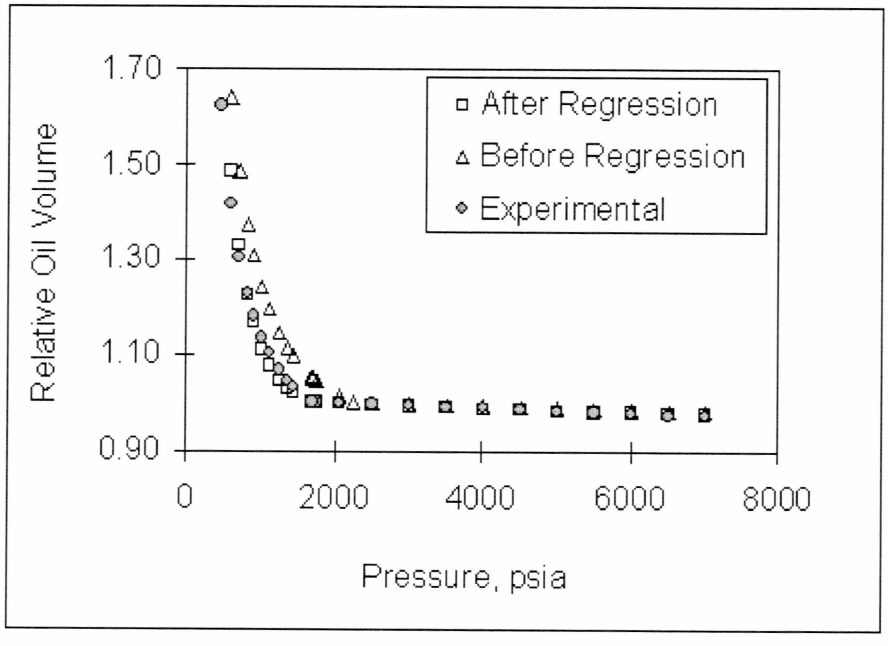

Figure 4.2: Relative oil volume before and after regression

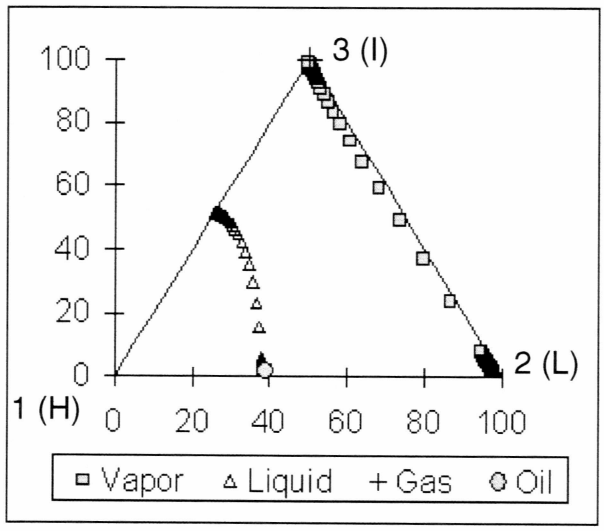

(a) 1600 psia

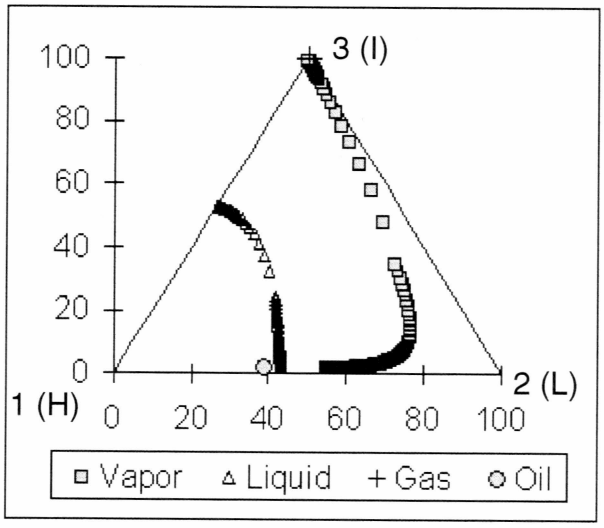

(b) 2600 psia

Figure 4.3 (a-b): Pseudo-ternary diagrams for West Sak Crude + CO_2 system where component 1: C_{7+} as the heavy fraction (H), component 2: N_2,C_1 as the light fraction (L), and component 3: C_2,C_3,C_4,C_5,C_6, and CO_2 as the intermediate fraction (I).

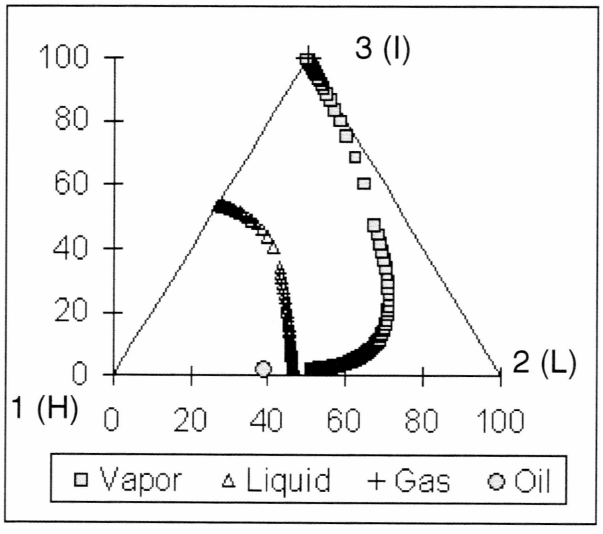

(c) 3600 psia

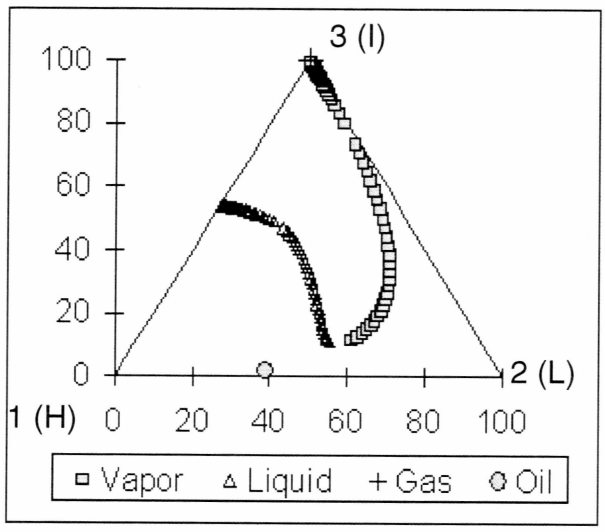

(d) 6600 psia

Figure 4.3 (c-d): Pseudo-ternary diagrams for West Sak Crude + CO_2 system where component 1: C_{7+} as the heavy fraction (H), component 2: N_2,C_1 as the light fraction (L), and component 3: C_2,C_3,C_4,C_5,C_6, and CO_2 as the intermediate fraction (I).

4.3 Simulation Results for Enhanced Viscous Oil Recovery by CO_2

On injection of pure CO_2 in the forty-acre five-spot injection pattern for 25 years, the oil rate in terms of STB/day was observed for each year. The OOIP for each PV injection case was 4.015 million STB. Occurrence of carbon dioxide breakthrough phenomenon for 10, 20, 30 and 50% of PV could be seen in Figures 4.4, 4.5, 4.6, and 4.7, respectively; the decrease in oil rate and increase in CO_2 flow rate clearly shows the onset of a breakthrough pattern in each PV injection scenario. For 50% PV injection, the gas breakthrough occurred after around 4.5 years into injection, which can be seen in Figure 4.7 as the beginning of a decrease in oil rate and increase in CO_2 rate. Similarly, Figure 4.6 shows the breakthrough after 6 years into injection. Figures 4.4 and 4.5 show a delayed occurrence of breakthrough for 10 and 20% PV. Table 4.2 lists the volume of CO_2 injected and produced for a 25-year injection period, at surface conditions of 60°F and 14.7 psia. The percentage recovery of OOIP increases as the amount of CO_2 injected increases, as can be seen in Table 4.2 and Figure 4.8, but along with an increase in percent recovery, storage ratio decreased. Gross utilization of CO_2, which is total CO_2 injected per barrel of oil produced, for 50% pore volume of CO_2 injection was found to be 9.709 Mscf/STB of oil produced. Additionally, increase in percent recovery will reach its plateau, where further increase in PV injected will not affect recovery, as can be observed in Figure 4.8.

Figures 4.5-4.7 show the sudden dip in the CO_2 flow rate after the breakthrough of CO_2. This could be attributed to an increase in the reservoir pressure due to continuous injection of CO_2, which could have led to the development of partial miscibility of incoming CO_2 with the West Sak oil. The incoming CO_2 tries to vaporize remaining heavier intermediate components due to increased reservoir pressure. This phenomenon could be observed as small increase in the oil rate after the breakthrough.

Table 4.2: Percentage recovery and CO_2 storage ratio at different PV

% PV	% Recovery	CO_2 Injected, million standard cubic ft	CO_2 Produced, million standard cubic ft	CO_2Storage Ratio
10	11.40	1.598	0.075	0.95
20	14.93	3.196	1.009	0.68
30	16.82	4.841	2.327	0.52
50	20.62	8.040	4.981	0.38

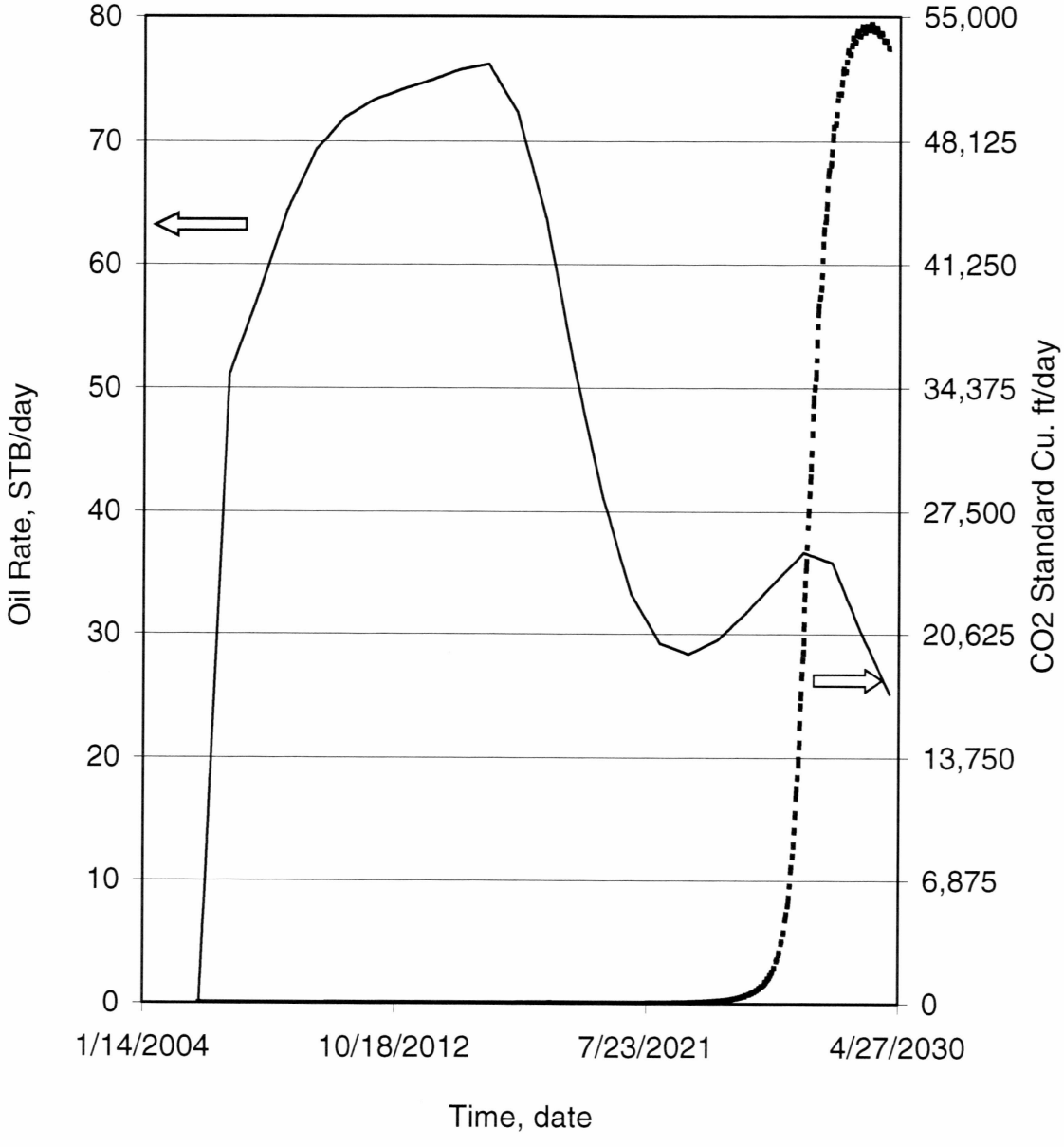

Figure 4.4: Changes in oil and CO_2 rate for 10% PV

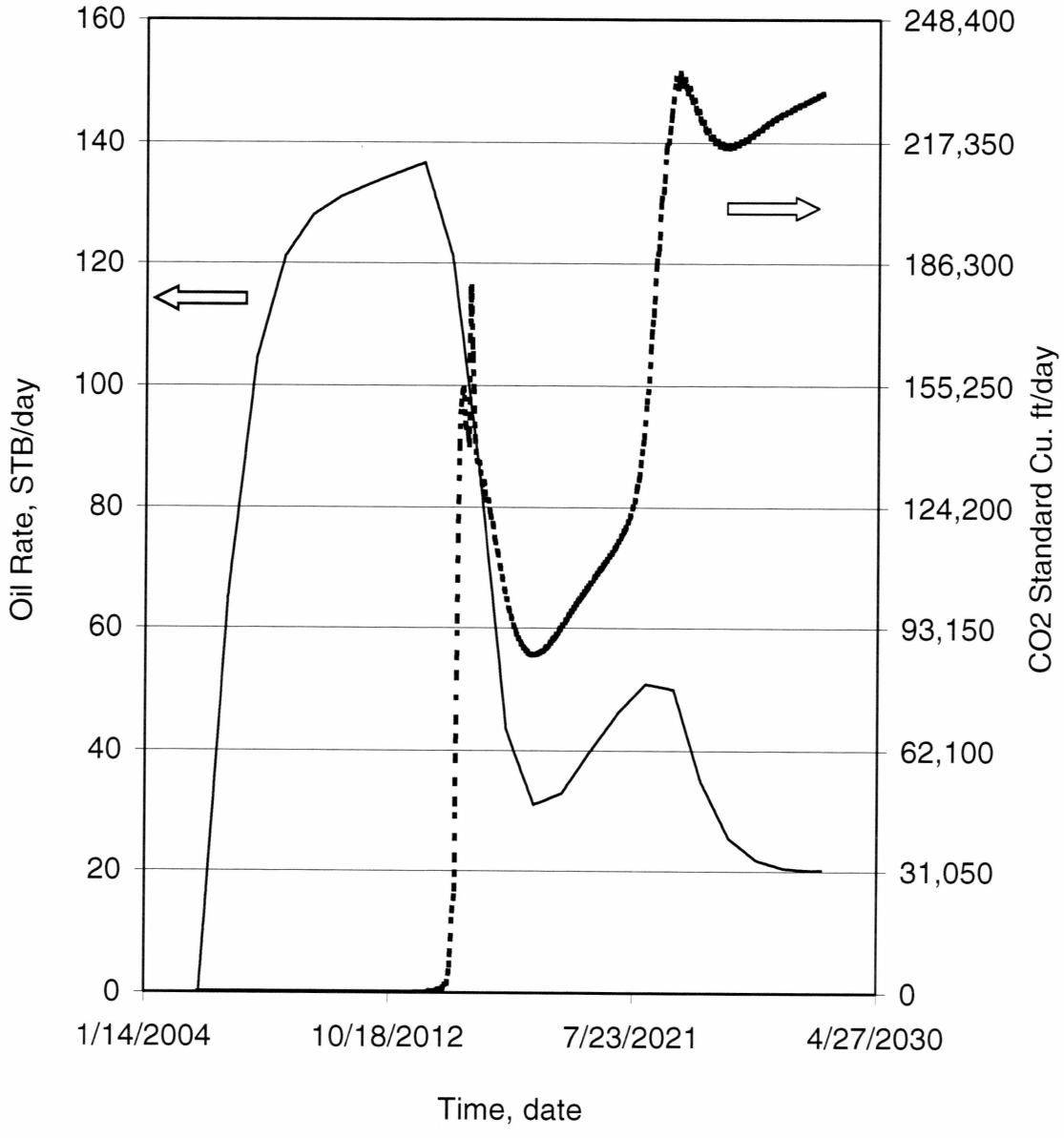

Figure 4.5: Changes in oil and CO_2 rate for 20% PV

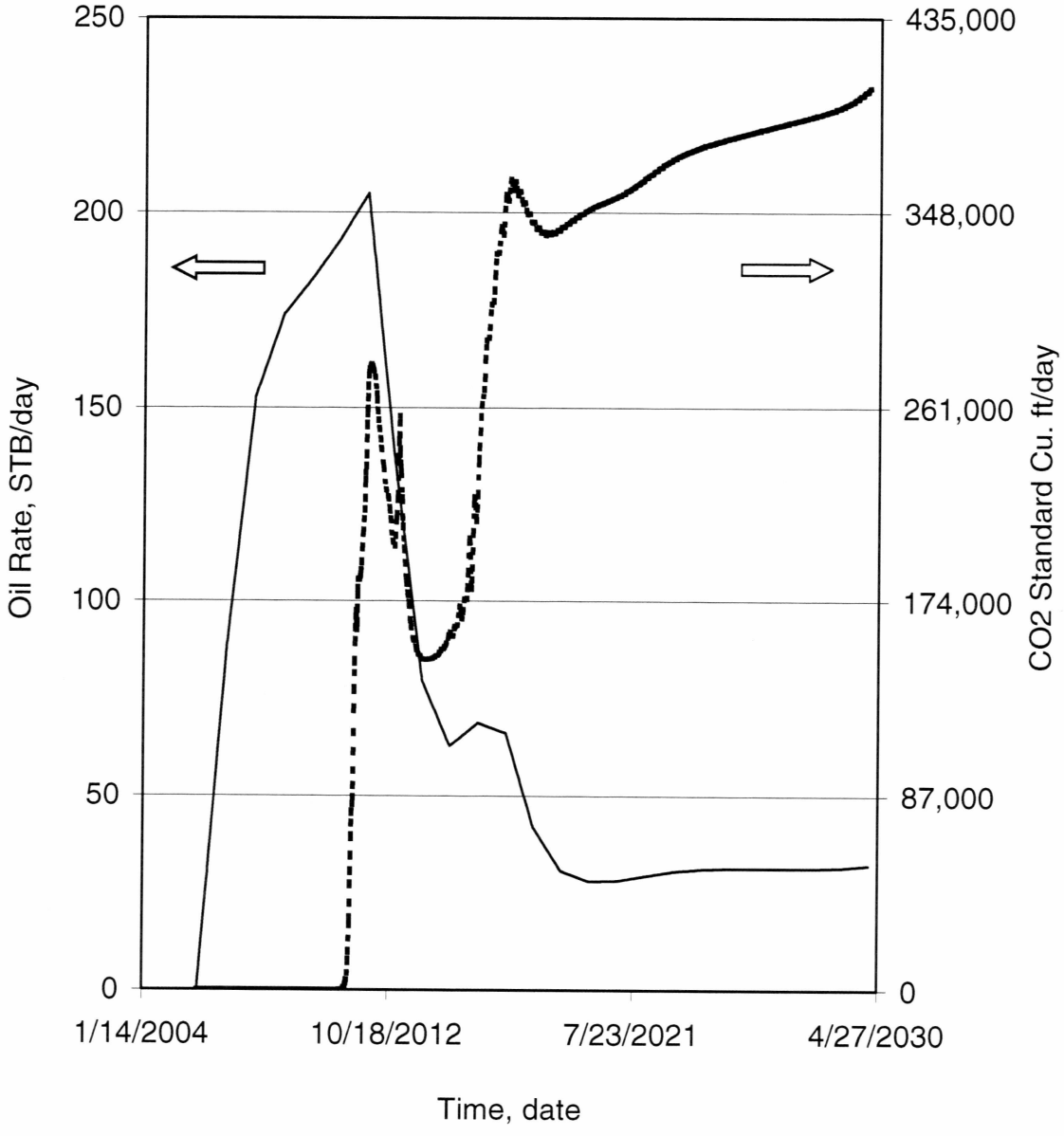

Figure 4.6: Changes in oil and CO_2 rate for 30% PV

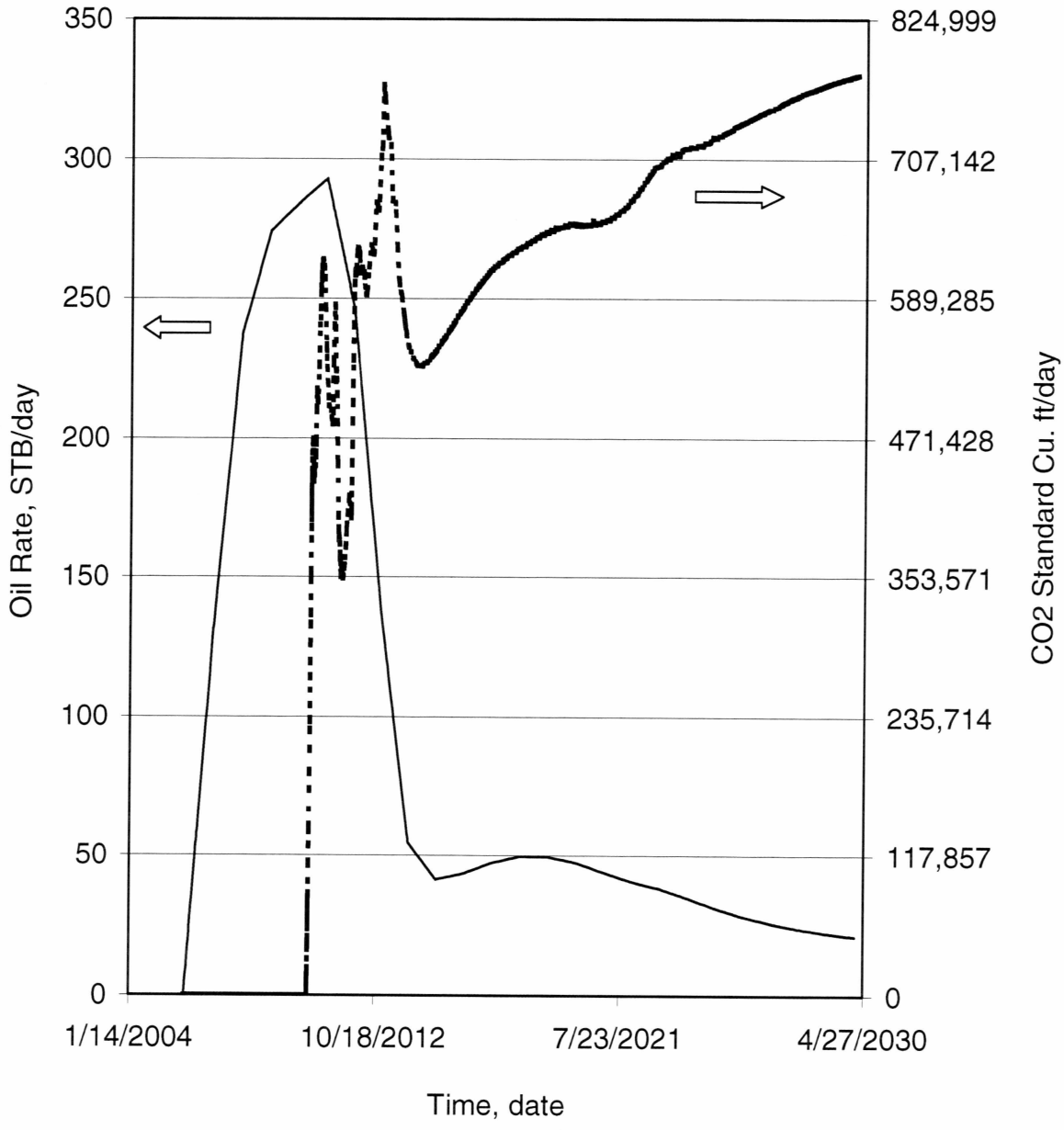

Figure 4.7: Changes in oil and CO_2 rate for 50% PV

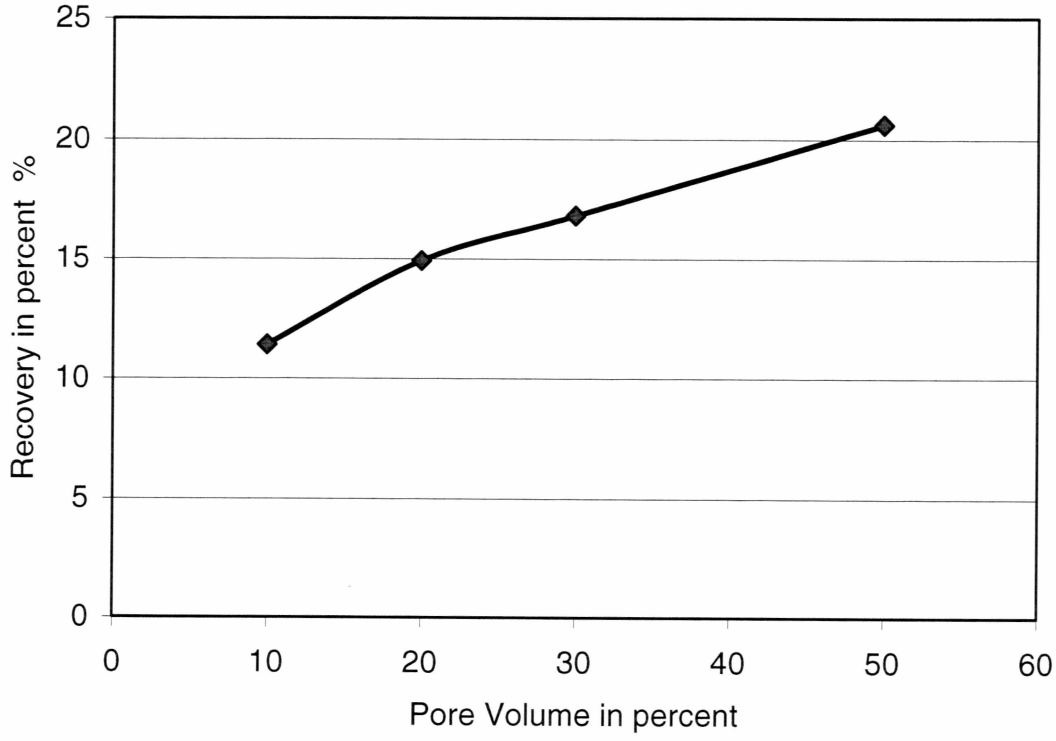

Figure 4.8: Percent of oil recovery versus injected PV

Figure 4.9 (a-d) illustrates the oil saturation profile for the 10% PV injection case at different time (t) intervals. Due to the size of the grid in this case, the oil saturation profile fails to show phenomenon of the viscous fingering, which is observed when the viscous phase is displaced by a lighter phase. Since the length of the viscous finger is smaller than the grid size of the model, the oil and CO_2 gas are assumed to mix instantly in each coarse grid block. The viscous fingering can be seen if the finer size grid system is selected, but it substantially increases the time and in turn the cost of simulation.

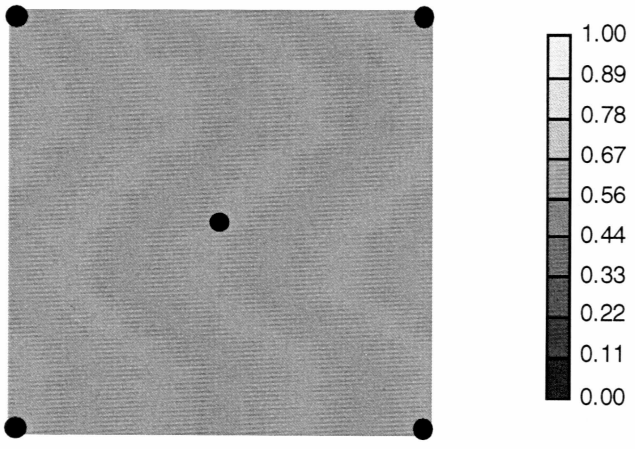

(a) t = 0 years

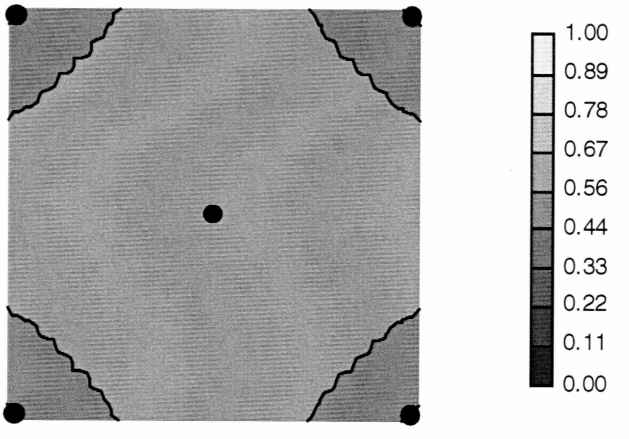

(b) t = 4 years

Figure 4.9 (a-b): Oil saturation profile for 10% PV injection

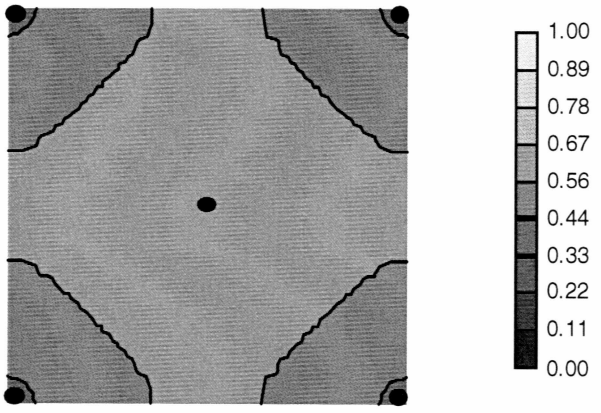

(c) t = 8 years

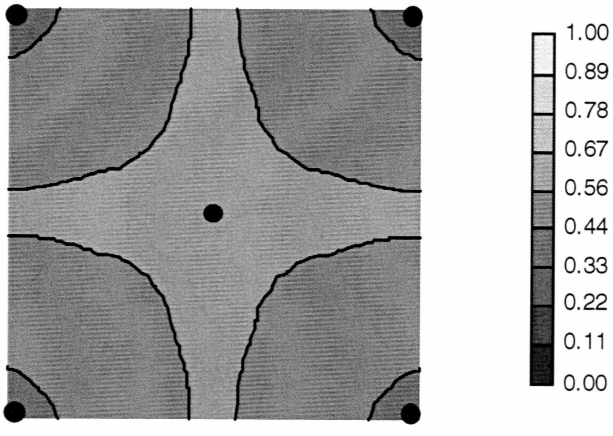

(d) t = 18 years

Figure 4.9 (c-d): Oil saturation profile for 10% PV injection

4.3 Economic Benefits and Incremental NPV of CO_2-EOR

Time value of the project, by calculating NPV, was used to evaluate the economical feasibility of CO_2-EOR. Comparison of NPV of CO_2-EOR with and without CO_2 credits was essential to understand how important the introduction of CO_2 credits to make CO_2 flooding projects economically successful. Figure 4.10 shows the comparison of NPV of the CO_2-EOR project with and without CO_2 credits. It was found that for 3000 acres CO_2-EOR, 1.37 million tons (average) of CO_2 per annum was injected and 38% of that injected CO_2 was stored in the reservoir formation. If the operating oil company were awarded US $10 for each ton of CO_2 stored, then for the 25 years project life with CO_2 credits, NPV would be US $26.90 million higher than that without CO_2 credits.

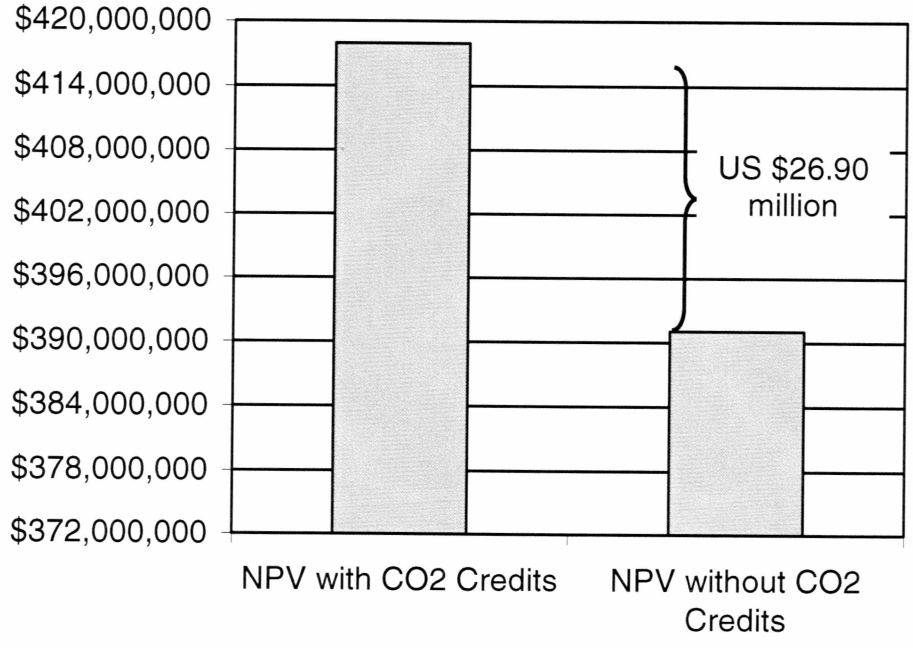

Figure 4.10: NPV with and without CO_2 credits

Sensitivity analysis of variables that influence NPV of the CO_2-EOR project is given in Figure 4.11. Figure 4.11 shows that an increase in market price of oil by US $1 could increase NPV by 45.5%, while an increase in the discount rate would decrease NPV by 52.3%. The CO_2 credits are the third influencing parameter after discount rate and oil price. Even though the CO_2 credits' impact on NPV is smaller, it can greatly increase NPV if higher CO_2 credits (more than US $10/ton of CO_2) are considered. Probability distribution (Figure 4.12) shows that the mean of NPV would be around US $0.44 billion. Figure 4.13 is plotted to demonstrate how the net present value would be affected if the oil price were increased from US $50 to 90 in $10 increments at discount rate ranging from 8% to 15%. As the value of the discount rate increased the NPV of CO_2-EOR project declined for each assumed oil price.

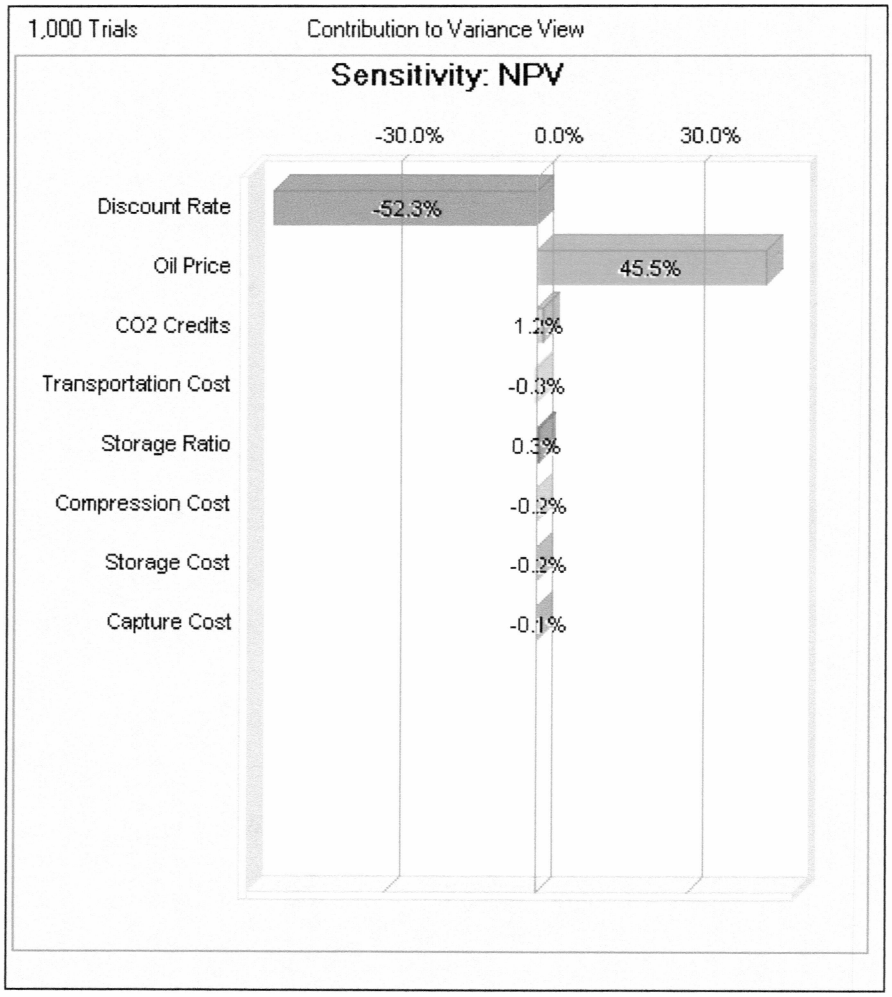

Figure 4.11: Sensitivity chart of input variables affecting NPV

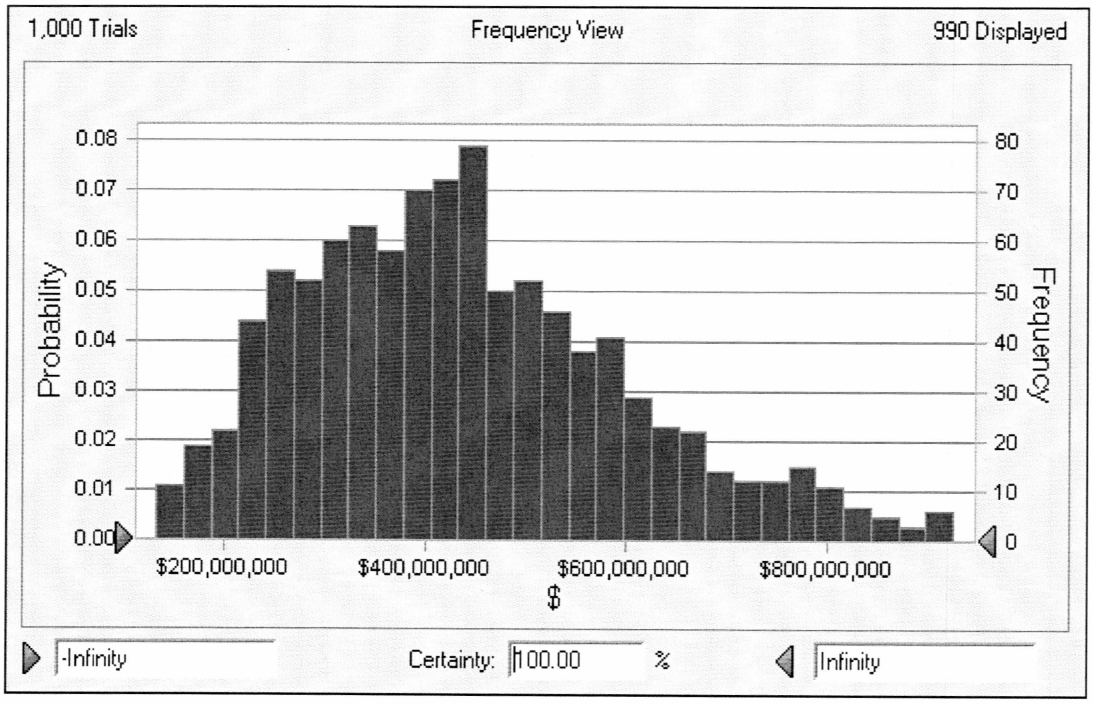

Figure 4.12: Probability distribution of NPV

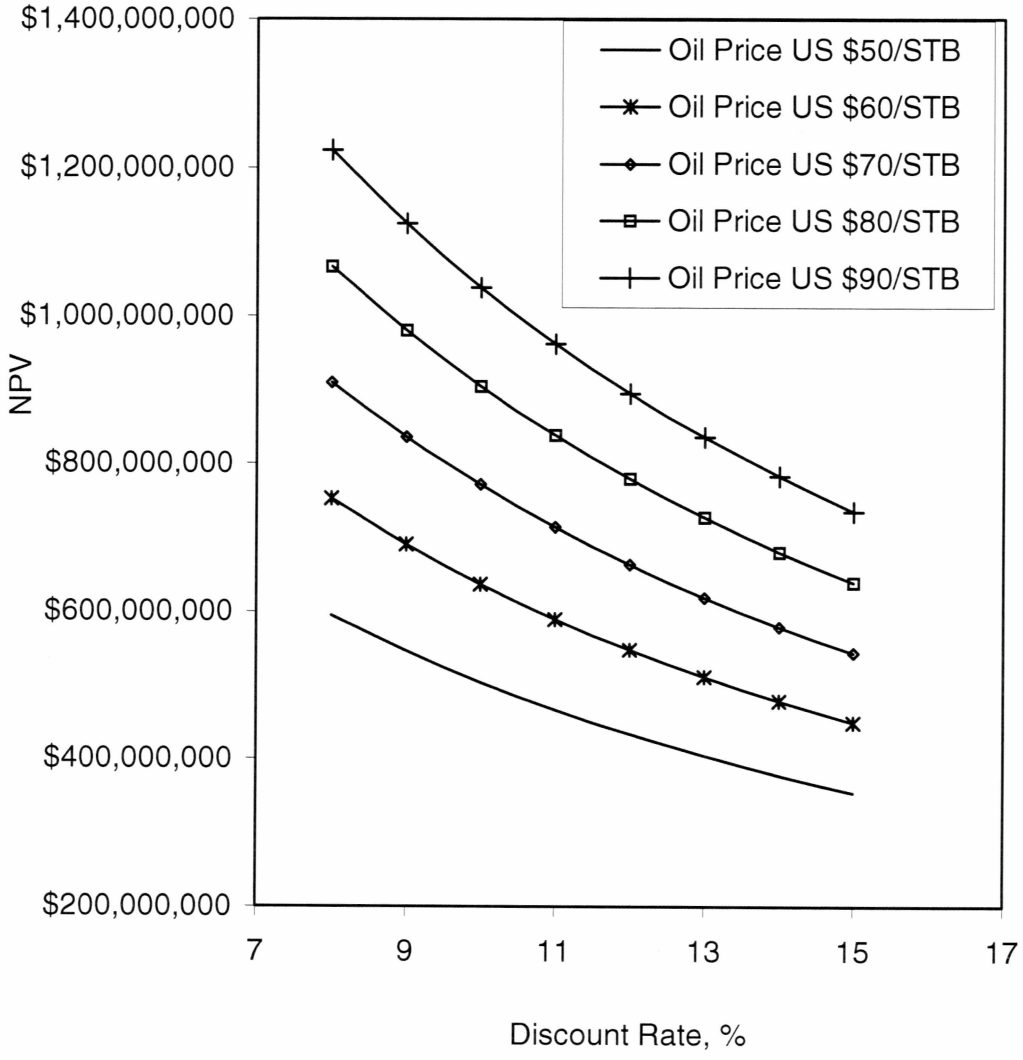

Figure 4.13: Net present value of the CO_2-EOR project for increasing oil prices with changing discount rate

4.5 Effect of CO_2 Storage on Saline Aquifer

To observe the effect of a CO_2 injection on a saline aquifer, a simulation study was carried out in STOMP®; 4.40 lb/sec of CO_2 was injected for a ten-year period. After simulating injection of CO_2 in a saline aquifer with STOMP®-WCSE, with assumed NaCl mass fraction of 0.05, at pressure of 2352 psia and 45°C (supercritical condition) in 2-D radial model, the changes in variables such as gas saturation, aqueous mass fraction, and temperature along the vertical distance were observed. Figures 4.14, 4.15, and 4.16 are plotted with above-mentioned variables on abscissa and vertical distance on ordinate at a radial distance of 280 ft from the injection point. Legends show the changes in variables at different time intervals for equal permeability values in the horizontal and vertical direction.

Figure 4.14 shows the carbon dioxide gas saturation at the time intervals of 500, 1000, 3650, and 7300 days. Up until the end of the injection period i.e. 3650 days, the gas saturation is increasing with increase in time, which is expected as injected gas moves along the radial distance. Ten years after the discontinuation of CO_2 injection, the gas saturation front starts receding as CO_2 gas moves vertically upward in the aquifer until it reaches a less permeable shale layer and gets trapped.

Dissolution of carbon dioxide gas, according to Henry's law, can be found as an aqueous mass fraction in Figure 4.15. In Figure 4.15, the mass fraction of CO_2 in

saline water follows the same trend as of gas saturation for 500 and 1000 days into injection, but as the time progresses the concentration of carbon dioxide in aqueous form increases in vertical direction as gas moves and gets dissolved in the upper layer. It is worth mentioning that leakage of CO_2 from layer 1 was zero, thus overlaying a less permeable layer provides seal against upwardly migrating CO_2.

Figure 4.16 illustrates the temperature profile for the same CO_2 injection scenario. Due to the supercritical nature of injected CO_2, the heat of the injection is transferred in a radial direction only along with movement of a supercritical gas, as can be seen in Figure 4.16, which represents the changes in the temperature profile in the saline aquifer region of the model. The geothermal temperature gradient in the permafrost region (from 0 to 4°C) remains the same at all time intervals.

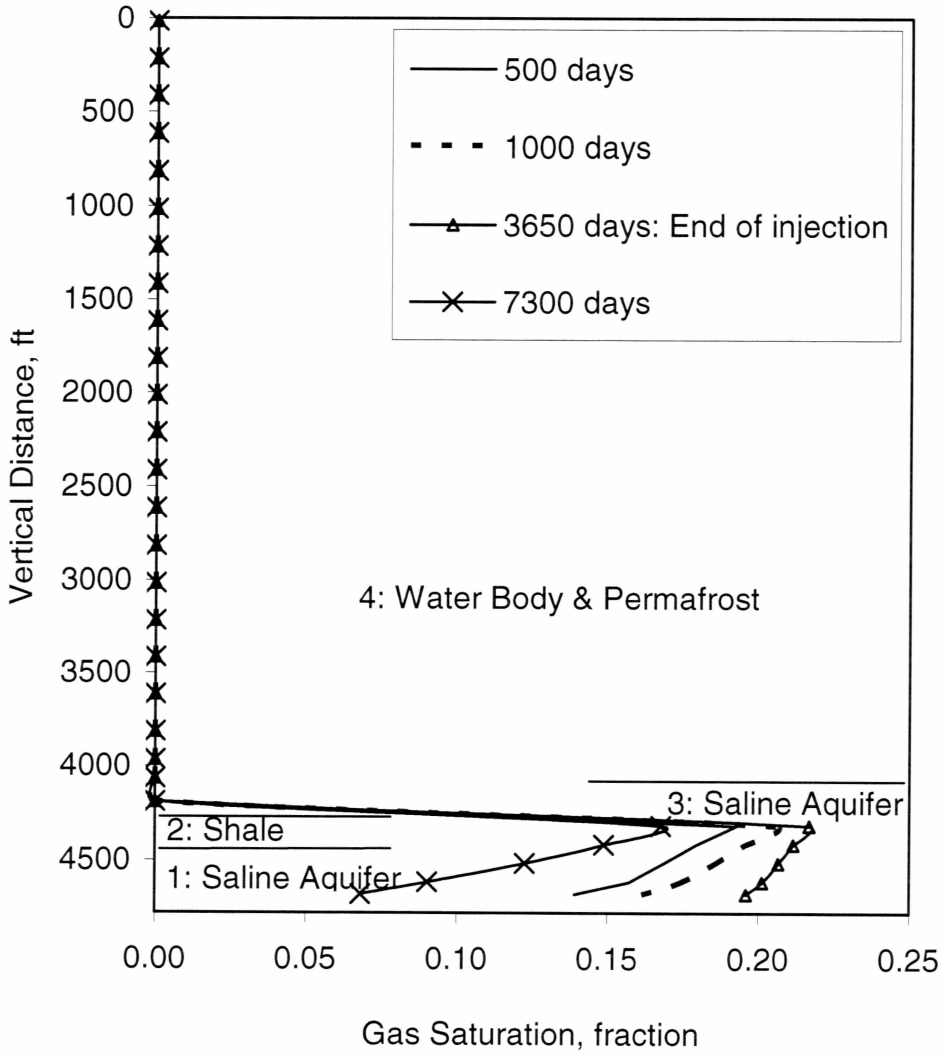

Figure 4.14: Gas saturation at horizontal distance of 280 ft from injection well

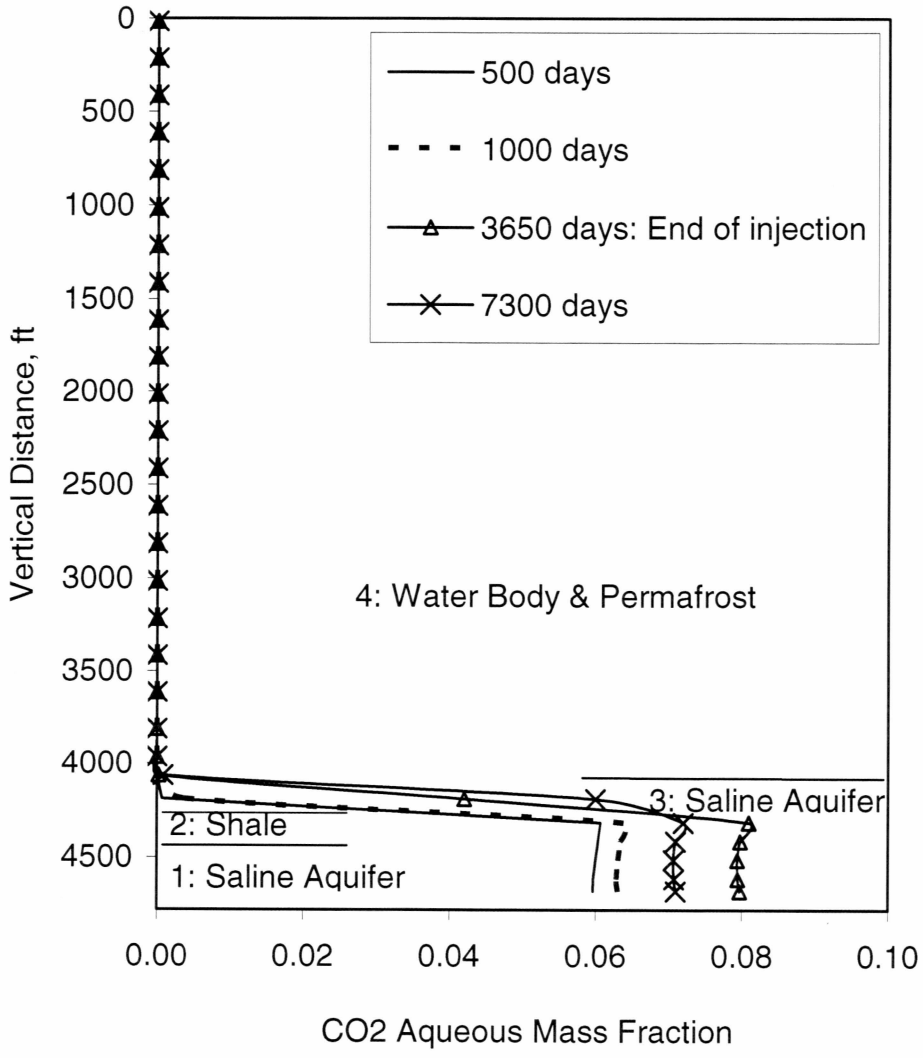

Figure 4.15: CO_2 aqueous fraction at horizontal distance of 280 ft from injection well

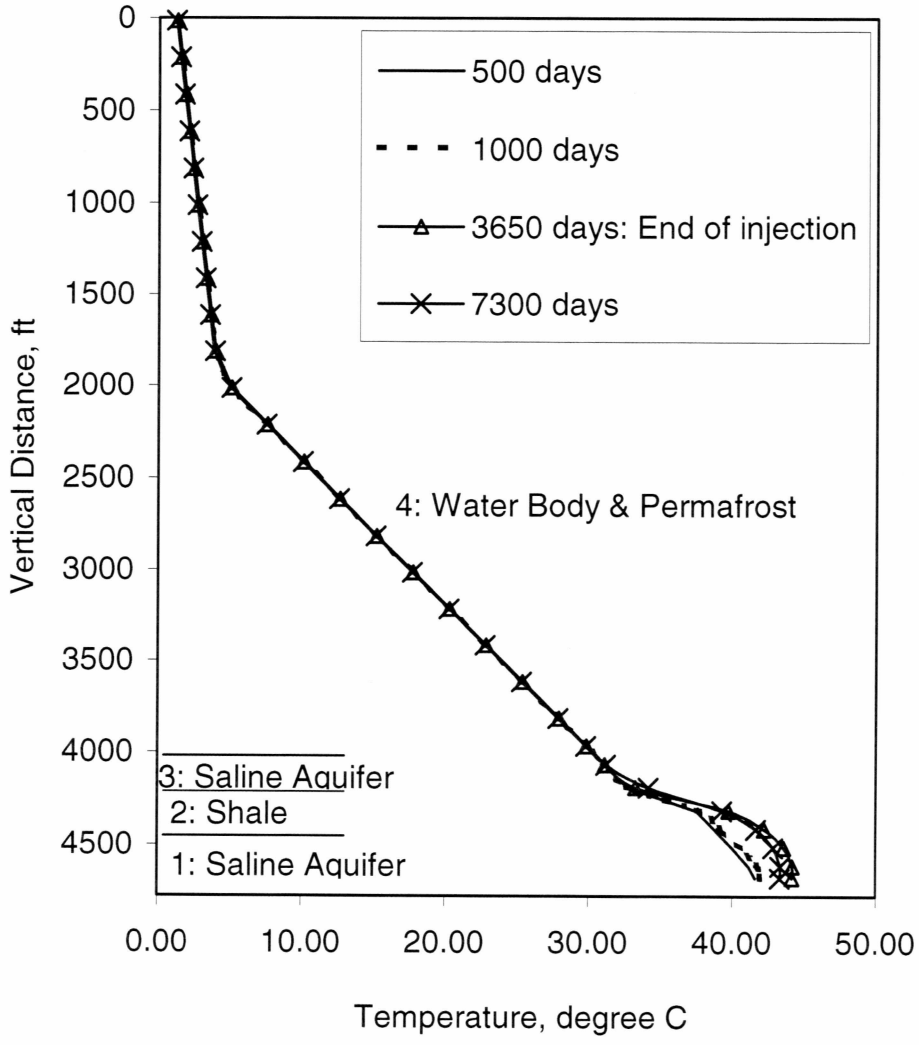

Figure 4.16: Temperature profile at horizontal distance of 280 ft from injection Well

Chapter 5

Conclusions and Recommendations

This chapter contains the conclusions derived from this study, in Section 5.1. Recommendations for future work are given in Section 5.2.

5.1 Conclusions

- Weight-assigned parameters such as temperature, pressure and average petrophysical properties of the oil pools are important to carry out rudimentary screening of potential oil pools on the ANS with respect to their amenability to CO_2-EOR.
- At reservoir pressures of the West Sak oil pool, the presence of partial miscibility can be observed from phase behavior study.
- Oil recovery by continuous CO_2 injection for 25 years predicted 20.62% oil recovery when 50% PV of CO_2 was injected. An increase in pore volume led to a decrease in CO_2 storage ratio.
- Economical analysis of CO_2-EOR proved to be important to estimate time value of the project. NPV of the project with CO_2 credits was found to be higher by US $26.90 million than NPV without CO_2 credits.
- At a rate of 4.40 lb/sec, a saline aquifer can successfully sequester CO_2 with no leakage. Changes in the temperature profile were negligible when

supercritical carbon dioxide was injected in a saline formation with NaCl mass fraction of 0.05.

5.2 Recommendations

Characterization of all Alaskan coalbeds, depleted oil, and gas pools could be performed to estimate the sequestration capacity and to screen out potential geological storage sites.

Complete characterization of the live West Sak oil could be helpful to describe a miscibility condition accurately. Due to the vast nature of the West Sak reservoir, a small pilot area for which the production history is available could be selected to perform compositional simulation and history matching.

There are many disposal wells on the ANS to inject generated waste into saline formation. Locations of these wells are chosen in such a way that there is no migration of fluids due to structural traps and faults. Formation physical properties of one such saline aquifer would be important to carry out simulation in STOMP® to simulate true migration of CO_2 gas and observe the temperature changes. Geo-chemical binding of CO_2 with rock could be predicted by developing a module in STOMP®, as chemical uptake of CO_2 over long-term is also crucial for sequestration studies.

Chapter 6

References

Abrishami, Y., Hatamian, H. and Dawe, R. A. 1997. Tuning of Peng-Robinson equation of state for simulation of compositional change in flue gas injection processes. Fluid Phase Equilibria, 139 (1): 219-254.

Ahmed, T. H. 1997. A generalized methodology for minimum miscibility pressure. Proceedings of the SPE Latin American and Caribbean Petroleum Engineering Conference, August 30-September 3, 1997, Rio de Janeiro, Brazil. Society of Petroleum Engineers, Inc., paper no. 39034.

Alaska Oil & Gas Conservation Commission (AOGCC). 2003. Annual Report (Revised on 6/8/04) [Online], [Cited February 26, 2006]. Available from: < http://www.state.ak.us/aogcc/annual/annindex.shtml >.

Allinson, G. and Nguyen, V. 2002. CO_2 geological storage economics. Proceedings of the Sixth International Conference on Greenhouse Gas Control Technologies, Japan: 615-620.

Bachu, S. and Stewart, S. 2002. Geological sequestration of anthropogenic carbon dioxide in the Western Canada sedimentary basin: Suitability analysis. Journal of Canadian Petroleum Technology, 41(2): 32-40.

Bachu, S. and Shaw, J. 2003. Evaluation of the CO_2 sequestration capacity in Alberta's oil and gas reservoirs at depletion and the effect of underlying aquifers. Journal of Canadian Petroleum Technology, 42 (9): 51-61.

Bakshi, A.K. 1991. Computer modeling of CO_2 stimulation in West Sak reservoir. M.S. Thesis, University of Alaska Fairbanks.

Bakshi, A.K., Ogbe, D.O., Kamath, V.A. and Hatzignatiou, D.G. 1992. Feasibility study of CO_2 stimulation in the West Sak field, Alaska. Proceedings of the Western Regional Meeting, March 30-April 1, 1992, Bakersfield, California, Society of Petroleum Engineers, Inc., paper no. 24038.

Benson, S. 2003. Geologic sequestration of carbon dioxide. [Online], [Cited July 12, 2006]. Available from:
< http://www.nap.edu/ openbook/0309089212/html/29.html>.

Bhandari, R. 1988. Prediction of phase behavior and miscibility conditions for West Sak crude-solvent mixtures. M.S. Thesis, University of Alaska Fairbanks.

Borchiellini, R., Massardo, A.F. and Santarelli, M. 2002. Carbon Tax vs. CO_2 effects on environmental analysis of existing power plants. Energy Conversion and Management, 43 (9-12): 1425-1443.

Bossie-Cordreanu, D and Gallo, Y.L. 2004. A simulation method for the rapid screening potential depleted oil reservoirs for CO_2 sequestration. Energy, 29 (9-10): 1347-1359.

Brush, R.M., Davitt, H.J., Aimar, O.B., Jorge Arguello, S.A. and Whiteside, J.M. 2000. Immiscible CO_2 flooding for increased oil recovery and reduced emissions. Proceedings of the SPE/DOE Improved Oil Recovery Symposium, Tulsa, Oklahoma, April 3-5, 2000, Society of Petroleum Engineers, Inc., paper no. 59328-MS.

Coats, K.H., and Smart, G.T. 1986. Application of a regression-based EOS PVT program to laboratory data. SPE Reservoir Engineering 1(3), Society of Petroleum Engineers, Inc., paper no. 11197: 277-299.

Dahowski, R. T., Dooley, J.J., Brown, D. R. and Stephan, A.J. 2001. Economic screening of geologic sequestration options in the United States with a carbon management Geographic Information System. Proceedings of the Eighteenth Annual International Pittsburgh Coal Conference, December 3-7, 2001, Newcastle, NSW, Australia.

Danesh, A.1998. PVT and phase behavior of petroleum reservoir fluids (Developments in Petroleum Science). Elsevier Science.

Doleschall et al.1999. Complex study of CO_2 flooding in Hungary. Miscible Gas Displacement, 299-311.

Domitrović, D., Šunjerga,S. and Jelić-Belta, J. 2004. Numerical solution of tertiary CO_2 injection at Ivanić oil field, Croatia. Proceedings of the SPE/DPE Fourteenth Symposium on Improved Oil Recovery held in Tulsa, Oklahoma, April 17-21, 2004, Society of Petroleum Engineers, Inc., paper no. 89361.

Energy Information of Administration (EIA). 2001. State energy-related carbon dioxide emissions by energy sectors. [Online], [Cited 30 June 2006]. Available from:
<http://www.eia.doe.gov/oiaf/1605/ggrpt/pdf/appc_tbl2.pdf>.

Energy Information of Administration (EIA). 2005. Emissions of Greenhouse Gases in the United States 2004, DOE/EIA-0573 (2004).

Gasper, A.T.F.S. Suslick, S.B., Ferreira, D.F. and Lima, G.A.C. 2005. Economic evaluation of oil production project with EOR: CO2 sequestration in depleted oil fields. Proceedings of the SPE Latin American and Caribbean Petroleum Engineering Conference, Rio de Janeiro, Brazil, June 20-23, 2005, Society of Petroleum Engineers, Inc., paper no. 94922.

Holm, W.L. 1987. Evolution of the carbon dioxide flooding processes. Journal of Petroleum Technology, 39(11): 1337-1342.

Holtz, M. H., Nance, P.K. and Finley, R.J. 1999. Reduction of greenhouse gas emissions through underground CO_2 sequestration in Texas oil and gas reservoirs [Online], [Cited 26 February 2006]. Available from: <http://www.beg.utexas.edu/environqlty/abndnhydrores/co2text.pdf>.

Klins, M.A. and Farouq Ali, S.M. 1981. Oil Production in shallow reservoirs by carbon dioxide injection. Proceedings of the Eastern Regional Meeting of the Society of Petroleum Engineers of AIME, Columbus, Ohio, November 4-6, 1981, paper no. 10374.

Klins, M.A. 1984. Carbon dioxide flooding: basic mechanisms and project design. International Human Resources Development Corporation.

Kovscek, A.R. 2002. Screening criteria for CO_2 storage in oil reservoirs. Petroleum Science and Technology 24 (7-8): 841-866.

Malik, Q.M. and Islam, M.R. 2000. CO_2 injection in the Weyburn field of Canada: optimization of enhanced oil recovery and greenhouse gas storage with horizontal wells. Proceedings of the SPE/DOE Improved Oil Recovery Symposium, Tulsa, Oklahoma, April 3-5, 2000. Society of Petroleum Engineers, Inc., paper no. 59327.

McGuire, P.L., Redman, R.S., Jhaveri, B.S. Yancey, K.E. and Ning, S.X. 2005. Viscosity reduction WAG: An effective EOR process for North Slope viscous oils. Proceedings of the SPE Western Regional Meeting, March 30-April 01, 2005, Irvine, California, Society of Petroleum Engineers, Inc., paper no. 93914.

Morgan, M.D. 2005. A model of Canadian oil and gas price fluctuations. Journal of Canadian Petroleum Technology, 44(7): 48-54.

Oostrom, M., Meck, D.H. and White, M.D. 2003. STOMP: SubsurfaceTransport Over Multiple Phases, Version 3.0 An Introductory Short Course. Prepared for the U.S. Department of Energy under Contract DE-AC06-76RL01830, Pacific National Laboratory.

Panda, M.N., Zhang, M., Ogbe, D.O., Kamath, V.A., and Sharma, G.D. 1989. Reservoir description of West Sak sands using well logs. Proceedings of the SPE California Regional Meeting, April 5-7, 1989, Bakersfield, California, Society of Petroleum Engineers, Inc., paper no.18759.

Peng, D. Y. and Robinson, D.B. 1976. A new two-constant equation of state. Ind. Eng. Chem. Fundam., 15: 59-64.

Pike, R. 2006. Technology tomorrow: The chemistry of carbon capture and storage. Journal of Petroleum Technology, June Issue, Editorial.

Pruess K., Xu, T., Apps, J. and Garcia, J. 2003. Numerical modeling of aquifer disposal of CO_2. Proceedings of the SPE/EPA/DOE Exploration & Production Environment Conference, San Antonio, TX, February 26-28, 2001, Society of Petroleum Engineers, Inc., paper no. 83695.

Research Institute of Innovative Technology for the Earth (RITE). 2004. Overview of the CO_2 Geological Sequestration System. [Online], [Cited 26 January 2006]. Available from: < http://www.rite.or.jp/English/lab/geological/geological.html>.

Rivas, O., Embid, S., and Bollvar, F. 1992. Ranking reservoirs for carbon dioxide flooding processes. SPE Advanced Technology Series 2(1), Society of Petroleum Engineers, Inc., paper no. 23641.

Robinson, D.B. and Peng, D. Y. 1978. The characterization of the heptanes and heavier fractions. Research Report 28, Gas Producers Association, Tulsa, Oklahoma.

Roper, M. 1989. An experimental study of CO_2 /West-Sak-crude-oil phase behavior. M.S. Thesis, University of Alaska Fairbanks.

Rubin, E.S. and Rao A.B. 2003. Uncertainties in CO_2 capture and sequestration costs. Proceedings of the 7th International Conference on Greenhouse Gas Control Technologies, 3: 1119-1124.

Saripalli, P.K., McGrail, B.P. and White, M.D. 2003. Modeling the sequestration of CO_2 in deep geological formations. Prepared for the U.S. Department of Energy under Contract DE-AC06-76RL01830, Pacific National Laboratory.

Sass, B., Gupta, N., Sminchal, J. and Bergman, P. 1998. Geochemical modeling to assess the capacity of a Midwestern United States geological formation for CO_2 sequestration. Greenhouse Gas Control Technologies: 1079-1086.

Saner, W.B. and Patton, J.T. 1983. CO_2 recovery of heavy oil: Wilmington field test. Proceedings of the SPE Annual Technical Conference and Exhibition, October 5-8, 1983, San Francisco, California, Society of Petroleum Engineers, Inc., paper no. 12082.

Senior, B., Adams, J., Espie, T., and Wright, I. 2004. Investigation of capture and storage could evolve as a large scale CO_2 mitigation option. Proceedings of the 7th International Conference on Greenhouse Gas Control Technologies, September 5-9, 2004, Vancouver, Canada.

Shan, C. and Pruess, K. 2004. EOSN-a new TOUGH2 module for simulating transport of noble gases in the subsurface. Geothermics, 33: 521-529.

Shaw, J. and Bachu, S. 2002. Screening, evaluation, and ranking of oil reservoirs suitable for CO_2-flood EOR and carbon dioxide sequestration. Journal of Canadian Petroleum Technology, 41 (9): 51-61.

Skovholt, O. 1993. CO_2 Transportation System. Energy Conversion and Management, 34(9-11): 1095-1103.

Srivastava R.K., Huang S.S., Dyer S.B. and Mourits F.M. 1995. Quantification of asphaltene flocculation during miscible CO_2 flooding in the Weyburn reservoir. Journal of Canadian Petroleum Technology, 34: 31-42.

Stalkup, F.I. 1984. Miscible displacement. Society of Petroleum Engineers of AIME. New York: Henry L. Doherty Memorial Fund of AIME.

Stalkup, F.I. 1987. Displacement behavior of the condensing/vaporizing gas drive process. Proceedings of the SPE Annual Technical Conference and Exhibition, September 27-30, 1987, Dallas, Texas Society of Petroleum Engineers, Inc., paper no. 16715.

Summerfield, I.R., Goldthorpe, S.H., Williams, N. and Sheikh, A. 1993. Costs of disposal options. Energy Conversion and Management, 34(9-11): 1105-1112.

Taber, J.J., Martin, F.D. and Seright, R.S. 1997. EOR screening criteria revisited- Part 1: Introduction to screening criteria and enhanced recovery projects field projects. SPE Reservoir Engineering 12(3), Society of Petroleum Engineers, Inc., paper no. 35385: 189-198.

Takur, G.C. and Sattar, A.1998. Integrated waterflood asset management. Tulsa, OK: Penn Well Publishing Company.

Van der Meer, L.G.H. 1996. Computer modeling of underground CO_2 storage. Energy Convers. Mgmt., 37(6-8): 1155-1160.

Werner, M.R. 1987. West Sak and Ugnu Sands: Low gravity oil zones on the Kuparuk River area, Alaskan North Slope. Alaskan North Slope Geology, 1:109-118.

White, M.D. and Oostrom, M. 2003. STOMP-Subsurface Transport Over Multiple Phases. Prepared for the US Department of Energy under Contract DE-AC06-76RLO 1830.

Zick, A.1986. A combined condensing/vaporizing mechanism in the displacement of oil by enriched gases. Proceedings of the SPE Annual Technical Conference and Exhibition, October 5-8, 1986, New Orleans, Louisiana. Society of Petroleum Engineers, Inc., paper no. 15493.

Appendix A

Lumping of Components and Tuning of EOS in CMG-WinProp®

The step-by-step procedure for lumping oil components, followed by tuning of EOS, in CMG-WinProp is given below with an example of the West Sak oil.

1. On launching WinProp® in CMG, in titles/EOS/units section, first EOS is chosen from four available EOS models. The four EOS models are Peng-Robinson (1978), Peng-Robinson (1976), and Soave-Redlich-Kwong (SRK) with proposed constant by Graboski and Daubert, and original SRK. For phase behavior study of West Sak oil, Peng-Robinson (1978) was selected, which is referred as PR-EOS (1978) in this study. For units, pressure and temperature of the system were set to psia and degree F, respectively, with component composition set to mole.
2. In component selection section, component and their properties can either be manually entered or selected from the array of hydrocarbon-nonhydrocarbon-component library, which can be performed by selecting **Insert library component** from the **Options** of the **Component definition** window. For the single-carbon-number hydrocarbons, for example C_6-C_{20}, components **FC_6-FC_{20}** can be selected from the component library. In the case of West Sak oil, 23 components (Bhandari, 1998) were selected from the library. Properties of heavy components (molecular weight of C_{21+} for West Sak oil) could be changed as per the available experimental values.

3. For West Sak oil, molar compositions of 23 components were entered in the composition section.
4. To group components according to the requirement of study, the **Component Lumping** option, available from **Characterization** of the menu, is invoked. In the lumping scheme window, 23 components of the West Sak oil were transformed into eight-component oil. CO_2 was set as a single group by assigning it number 1 in the scheme column, and combining methane and nitrogen as a second group, assigning each component number 2 in the scheme column. Similarly, C_2-C_6 components were lumped as a third group, and then C_{7+} fractions were grouped into five pseudo-components. By clicking on **OK**, the components are lumped together. In the **File** option from the menu, the properties of the components should be updated after lumping (Using **Update component properties**). This must be followed by deleting lumping option from the main window before starting tuning of EOS by regression.
5. The advantages of using lumping in this study were to have more flexibility with the selection of regression parameters for tuning of EOS and to reduce the compositional simulation run time in GEM®.
6. To tune EOS, the regression feature of WinProp® can be used. The experimental data is matched with values predicted by EOS by selecting regression parameters, which are properties of the component and interaction coefficients. First **Regression** option from menu is invoked to begin selection

of regression parameters. To tune PR-EOS (1978) for the West Sak oil, the critical properties and acentric factors of components C_7 through C_{21+}, omega A and B parameters for methane and C_{21+}, viscosity parameters, and interaction coefficients are used as the regression parameters. These parameters are selected by clicking on the respective grids of the properties of components.

7. Experiments for EOS tuning are entered by invoking **Lab** options of the menu. Constant composition expansion and differential libration experimental data, obtained from Roper (1988), was used to tune PR-EOS (1978). Weights are assigned according to importance and reliability of the experimental data to the tuning. For example, the saturation pressure was assigned weight of 50, while the volumetric analysis and viscosity of the oil was given weight of 7 and 40, respectively.
8. Once the experimental data are entered, end of regression should be invoked by selecting **End of Regression** from **Regression** of the menu. Then regression scenario is run to obtain tuned parameters of EOS. Subsequently, the tuned EOS is used for performing other phase behavior calculations.